AGU ADVANCING EARTH AND SPACE SCIENCE

Water Resources Research

RESEARCH ARTICLE
10.1029/2020WR028046

Logjams and Channel Morphology Influence Sediment Storage, Transformation of Organic Matter, and Carbon Storage Within Mountain Stream Corridors

Nicholas A. Sutfin[1,2], Ellen Wohl[1], Timothy Fegel[3], Natalie Day[4], and Laurel Lynch[5]

[1]Department of Geosciences, Colorado State University, Fort Collins, CO, USA, [2]Integrated Water, Atmosphere, and Ecosystem Education and Research Program, Colorado State University, Fort Collins, CO, USA, [3]Rocky Mountain Research Station, United States Forest Service, Fort Collins, CO, USA, [4]Department of Zoology and Physiology, University of Wyoming, Laramie, WY, USA, [5]Department of Soil and Water Systems, University of Idaho, Moscow, ID, USA

Key Points:

- Less-confined valleys store relatively more carbon per area in floodplain fine sediment and large wood than more confined valley segments
- Within wide valleys, channels with single-thread planforms store more carbon than more complex systems with multiple channels of flow
- Logjam abundance is linked to microbial transformation of organic matter and shallower fine sediment depth in complex multithread reaches

Supporting Information:

Supporting Information may be found in the online version of this article.

Correspondence to:

N. A. Sutfin,
nicksutfin@gmail.com

Citation:

Sutfin, N. A., Wohl, E., Fegel, T., Day, N., & Lynch, L. (2021). Logjams and channel morphology influence sediment storage, transformation of organic matter, and carbon storage within mountain stream corridors. *Water Resources Research*, *57*, e2020WR028046. https://doi.org/10.1029/2020WR028046

Received 28 MAY 2020
Accepted 28 APR 2021

Abstract The flow of organic matter (OM) along rivers and retention within floodplains contributes significantly to terrestrial carbon storage and ecosystem function. The storage and cycling of OM largely depend upon hydrogeomorphic characteristics of streams and valleys, including channel geometry and the connectivity of water across and within the floodplain. To examine the role of river morphology on carbon dynamics in mountain streams, we (a) quantify organic carbon (OC) storage in fine sediment, litter, and wood along 24 forested gravel-bed stream reaches in the Rocky Mountains of CO, USA, (b) examine morphological factors that regulate sediment and OC storage (e.g., channel width, slope, logjams), and (c) utilize fluorescence spectroscopy to examine how the composition of fluorescent dissolved OM in surface water and floodplain fine sediment are influenced by channel morphology. Multivariate regression of the study reaches, which have varying degrees of confinement, slope, and elevation, indicates that OC storage per area is higher in less confined valleys, in lower gradient stream reaches, and at higher elevations. Within unconfined valleys, limited storage of fine sediment and greater microbial transformation of OM in multithread channel reaches decreases OC storage per area (252 ± 39 Mg C ha^{-1}) relative to single-thread channel reaches (346 ± 177 Mg C ha^{-1}). Positive feedbacks between channel morphology and persistent channel-spanning logjams that divert flow into multiple channels may limit the aggradation of floodplain fine sediment. Although multithread stream reaches are less effective OC reservoirs, they are hotspots for OM decomposition and provide critical resources to downstream food webs.

Plain Language Summary Organic matter, in the form of byproducts of plants, insects, and microbes, is a critical component of healthy riverine ecosystems and contributes to carbon storage, which reduces carbon dioxide release to the atmosphere. To examine how the shapes of river channels and valleys influenced organic matter storage, we (a) surveyed 24 streams in the Colorado Rocky Mountains and collected soil samples to estimate carbon storage, (b) related differences in carbon storage to river morphology, and (c) examined how channel geometry influenced the molecular composition of dissolved organic matter. We found that carbon storage per area is higher in wider valleys, in lower gradient streams, and at higher elevations. Within wide valleys, streams with a single channel of flow stored more sediment and carbon than streams with numerous channels of flow. Complex river channels also increased the molecular transformation of carbon by microbial communities. Although complex river features are less efficient reservoirs for organic matter, they increase carbon availability to downstream food webs and play an important role in maintaining healthy ecosystems.

1. Introduction

Rivers play a significant role in terrestrial carbon budgets through release of organic carbon (OC) to the atmosphere, delivery to oceans (Aufdenkampe et al., 2011; Galy et al., 2015), and storage in downed, dead wood, and floodplain soil (Sutfin et al., 2016). Combined OC storage in the atmosphere and biosphere is less than storage in soils (Falkowski et al., 2000), which have the potential to retain OC at depth along river corridors (Ricker & Lockaby, 2015; D'Elia et al., 2017; Omengo et al., 2018). Because the highest uncertainty

in annual exchanges of carbon between the atmosphere, surface ocean, and land surface occurs within terrestrial reservoirs (Ballantyne et al., 2012; Gregory et al., 2009), OC dynamics and storage along river floodplains could represent a substantial component of global carbon budgets.

Although large, lowland rivers have extensive floodplains that can store OC (Hoffmann et al., 2009; Hupp et al., 2019; Lininger et al., 2019), smaller streams constitute ~95% of global river length and may disproportionately influence OC cycling (Downing et al., 2012). Allochthonous (terrestrially derived) organic matter (OM) inputs in headwater streams are the foundation of food webs, and are crucial for fisheries and autochthonous (in-stream) primary production in larger rivers (Chapin et al., 2011; Vannote et al., 1980). Herein, we use OC when discussing storage reservoirs of OC (Mg C ha^{-1}) and OM when discussing specific sources of OC and the decomposition or transformation of those sources by microbial communities and aquatic invertebrates. Floodplains along first, second, and third order mountainous headwater streams have been shown to contain higher soil OC content than adjacent uplands (Sutfin & Wohl, 2017; Wohl et al., 2012) and can store more OC per area than higher order lowland rivers (Sutfin et al., 2016). We focus on these smaller streams to examine controls on OC dynamics within river corridors.

Determining whether OC retention within floodplains constitutes long-term C storage requires considering (a) the duration of floodplain fine sediment storage prior to downstream transport, and (b) the potential for OC losses to the atmosphere via decomposition and mineralization of OM. Geomorphic response to floods regulates the duration of sediment storage (Sutfin & Wohl, 2019), while hydrologic connectivity regulates decomposition of OM (Raymond et al., 2016; Wollheim et al., 2018). Thus, the potential for OC storage along river corridors is highly sensitive to hydrological condition, and valley and channel geometry.

Biophysical factors that influence channel geometry and hydrologic connectivity include in-stream wood, logjams, beaver ecosystem engineering, vegetation, valley width and confinement, and hydrologic flow and sediment regimes, which together create and maintain channel complexity (Livers & Wohl, 2016; Polvi & Wohl, 2013). Here, channel complexity captures the presence and variability of diverse channel geometry, including planform and bedforms. Greater channel complexity equates to increased spatial variability in channel geometry (Livers & Wohl, 2016). Increased channel complexity is more common along headwater streams, as a result of limited human impact and prevalent biotic drivers of channel morphology (i.e., logjams, beavers) (Beckman & Wohl, 2014; Polvi & Wohl, 2013). While complex headwater streams may have a higher capacity to store OC (Sutfin et al., 2016; Wohl et al., 2012), they may also act as hotspots of OM decomposition, where longer water residence times (Gooseff et al., 2007) provide greater opportunities for microbial metabolism (Battin et al., 2008). Recent work shows that the composition of OM flowing through complex channel segments is more molecularly diverse than that of single-thread channels; these differences become increasingly pronounced as seasonal declines in flow reduce hydrologic connectivity across the floodplain (Lynch, Sutfin, et al., 2019). The degree to which higher channel complexity corresponds to enhanced OC storage versus decomposition and mineralization, however, remains poorly constrained.

Here, we (a) quantify differences in OC storage per area along valley segments with varying channel and valley geometry, (b) identify potential hydrogeomorphic mechanisms underlying differences in OC storage, and (c) examine longitudinal trends in the composition of OM, as it cycles through surface waters and adjacent floodplains. To quantify OC storage, we surveyed and sampled 24 relatively undisturbed study reaches with similar geology (Braddock & Cole, 1990) and climate (Birkeland et al., 2003), spanning an ecotone and vegetation shift (Polvi et al., 2011; Veblen & Donnegan, 2005) along the tributaries and main stem of four headwater streams within the South Platte River basin in northern Colorado. Six years of logjam presence surveys at nine of the 24 study reaches complement morphology surveys to examine the role of logjams on sediment and OC storage. Two of the 24 study reaches were extended in length, creating intensive study sites that we used to investigate the role of channel geometry and logjams on OM transformation in surface waters and floodplain fine sediment. Although we focus on the details of OM and OC dynamics in small streams of the Southern Rockies, USA, the along-stream variations in channel and valley morphology and hydroclimatology that occur in the study area are common in mountainous regions (Wohl, 2013b). In addition, diverse human activities throughout the temperate latitudes have caused widespread simplification of headwaters and lowland rivers (Brown et al., 2018), thus reducing the complexity that strongly influences OM transformations. Consequently, the research summarized here has broad implications for

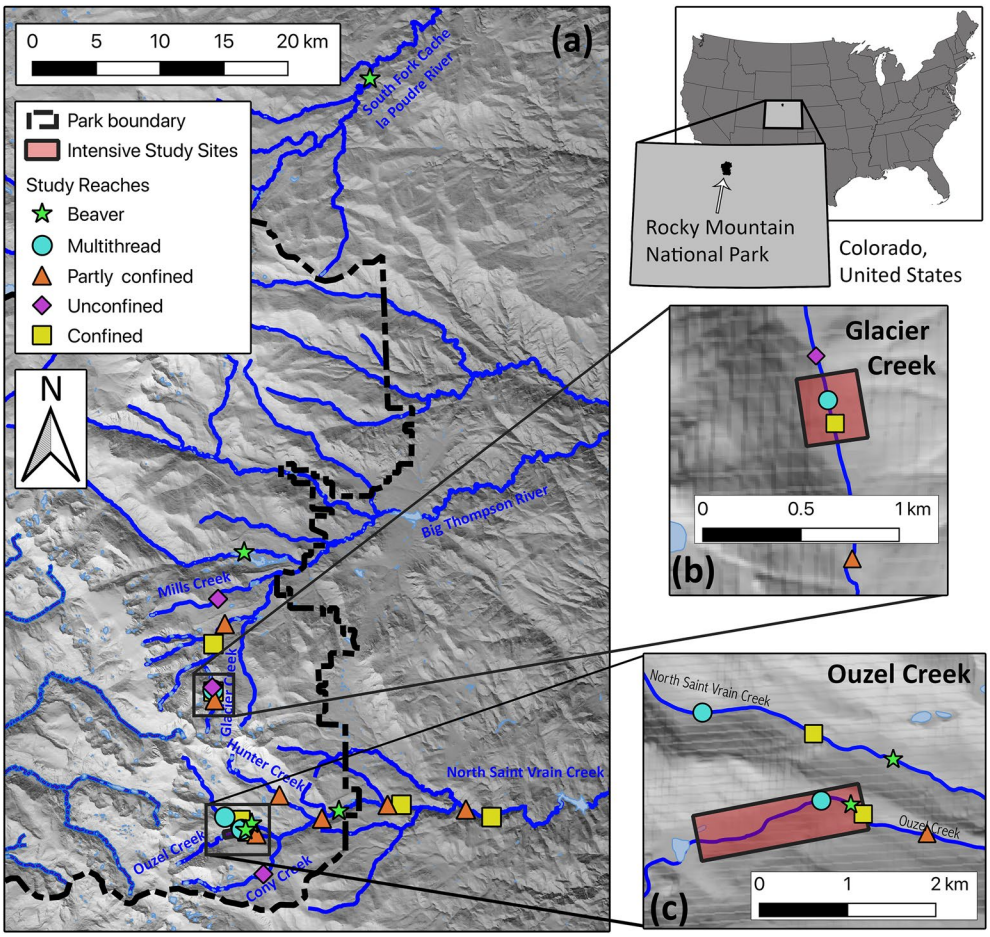

Figure 1. Map of the study area along the Colorado Front Range of the Rocky Mountains, U.S. The 24 study reaches representing five different channel types (a) are defined in the legend. Large rectangles with bold outlines identify intensive study sites that capture transitions in the channel complexity (single-multiple-single thread reaches) on GCK (b) and Ouzel Creek (c). At these intensive study sites, organic matter composition was examined along transitions in valley confinement using fluorescence spectroscopy. Logjam surveys were conducted in the North Saint Vrain Creek Basin upstream of the Rocky Mountain National Park boundary.

carbon dynamics across unaltered and highly impacted streams that can inform river restoration and land management decisions.

2. Study Area

At sites within and around Rocky Mountain National Park and the Arapaho and Roosevelt National Forests, we surveyed 24 study reaches in the subalpine and montane zones of nested tributaries within the North Saint Vrain Creek (NSV), Glacier Creek (GCK), South Fork of the Poudre River (SFP), and Big Thompson River (BTR) watersheds (Figure 1). Smaller tributaries surveyed also include Ouzel, Cony, Hunters, and Mills Creeks

2.1. Geological Setting

The geology and glacial history within the Colorado Front Range (CFR) of the Rocky Mountains regulates valley morphology in the study area but does not directly influence OC inputs to the study reaches. The underlying lithologic core of the CFR is composed of Precambrian gneiss, schist, granite, and other igneous rocks primarily of intrusive origin (Braddock & Cole, 1990). Irregular bedrock jointing facilitates longitudinal variability in the relative confinement of stream valleys, such that broader valleys commonly coexist

with more closely spaced bedrock joints and strath terraces along otherwise confined, narrower valleys (Wohl, 2008). Pleistocene alpine terminal moraines extend eastward downvalley to elevations of ~2,300–2,500 m and play a significant role in shaping the relative confinement of valleys among study reaches. On the eastern side of the CFR, knickpoints at ~2,000 m in elevation mark the downstream transition from broader glaciated valleys to narrow incised valleys in sedimentary rocks at the eastern margin of the Precambrian core (Anderson et al., 2006). Broader valleys typically have pool-riffle or plane bed channel morphology, whereas more confined valleys are more likely to have cascade or step-pool morphology, including both boulder and logjam-forced steps (Livers & Wohl, 2015; Montgomery & Buffington, 1997).

2.2. Climate and Vegetation

Distinct vegetation zones reflect differences in precipitation patterns and fire regimes (Veblen & Donnegan, 2005) that influence hydrologic flow paths and OM inputs to streams and floodplains. Vegetation in the study area reflects changes across the ecotone from montane to subalpine forests in the CFR. At 1,830 m elevation, grassland steppe vegetation transitions into montane forest, which is dominated by ponderosa pine (*Pinus ponderosa* var. *scopulorum*) and Douglas-fir (*Pseudotsuga menziesii*) extending to ~2,750 m. The montane zone receives ~75 cm of annual average precipitation in the eastern CFR (record spanning 1981–2010; PRISM Climate Group, 2012) and experiences relatively frequent and low severity ground fires approximately every 30–100 years (Veblen & Donnegan, 2005). Forests in the subalpine zone, extending from ~2,750 to 3,400 m, are dominated by subalpine fir (*Abies lasiocarpa*), lodgepole pine (*Pinus contorta*), limber pine (*Pinus flexilis*), Engelmann spruce (*Picea englemannii*), and aspen (*Populus tremuloides*) (Veblen & Donnegan, 2005). Large stand-replacing fires occur on average every 500 years in the subalpine zone, where annual average precipitation is ~85 cm (Barry, 1973; Birkeland et al., 2003; PRISM Climate Group, 2012). Vegetation within the riparian zone typically corresponds to that of respective upland vegetation with additions of blue spruce (*Picea pungens*). Willow (*Salix* spp.), sedges (*Carex* spp.), and river birch (*Betula fontinalis*) are present at sites with relict beaver activity (Polvi et al., 2011; Veblen & Donnegan, 2005). Active beaver meadows were formerly abundant, but are now restricted to a few sites in the study area (Wohl, 2013a).

2.3. Hydrological Condition

The rivers and streams of the CFR are snowmelt dominated and typically have a single annual hydrograph peak during June. Paleoflood indicators and estimates of flood magnitudes in the CFR (Jarrett, 1990; McCain & Shroba, 1979) suggest that high-intensity convective storms (typically from July to September), which occur at elevations below 2,300 m, disproportionately influence stream discharge at elevations within and below the montane zone. Hydrologic response to these storms sometimes results in secondary peak flows that exceed the snowmelt-dominated peak (Jarrett, 1990). One such event occurred during the period of this study.

On September 11–13, 2013, prolonged extreme rainfall broke several records in the State of Colorado (Gochis et al., 2014) and resulting floods restructured floodplains in much of the CFR (Sholtes et al., 2018; Yochum & Collins, 2015; Yochum et al., 2017). Estimated recurrence intervals of peak discharge in rivers and streams during the event ranged from 5 to >100-year flows (Yochum & Collins, 2015). Most of our study reaches were located outside the center of the highest rainfall accumulations and received somewhere between ~100 and 250 mm of rain, equating to 10 to 500 year precipitation events (Gochis et al., 2014). However, the lower portion of NSV was within the center of the storm and received ~380–520 mm of rainfall. Four study sites were heavily impacted.

Estimates of peak discharge in streams and rivers of the CFR during the 2013 storm do not include values for NSV at Allenspark, but estimates of sediment residence time provide context for the recurrence interval of the flood. The United States Geological Survey (USGS) stream gauge on NSV near Allenspark, CO (gauge # 6721500), downstream of 11 and upstream of 4 of our study reaches, was no longer active in 2013, but discontinuous records of flow (1926–1930, 1987–1997) indicate a daily mean annual discharge of 1.56 $m^3\ s^{-1}$ and a maximum annual peak discharge of 13.30 $m^3\ s^{-1}$. Yochum and Collins (2015) estimate that flow at the NSV Allenspark gauge was greater than a 2-year flood. However, radiocarbon ages of charcoal fragments in

floodplain fine sediment samples collected at two sites below the USGS Allenspark gauge before the flood suggested an estimated floodplain sediment residence time of ~600 years BP (Sutfin & Wohl, 2019). Erosion of floodplain fine sediment at these two study reaches during the 2013 flood suggests a recurrence interval >500 years. Preflood and post-flood lidar differencing and sediment coring of the Ralph Price Reservoir downstream quantified ~100 years of erosion along the lower NSV corridor and a substantial loss of OC storage during the flood (Rathburn et al., 2017).

Stream gauges in the study area lack continuous discharge data of sufficient length to estimate recurrence intervals with meaningful certainty, but can provide context for annual trends, seasonal patterns in discharge, and the magnitude of the 2013 event. The USGS gauge (#402114105350101) on the BTR at Moraine Park located downstream of eight of our study reaches and upstream of Estes Park provides 17 discontinuous years of streamflow between 1996 and 2020. This gauge recorded an annual mean of 1.6 $m^3 s^{-1}$ and a daily mean annual maximum of 17 $m^3 s^{-1}$ for the period of record. Annual peak flows within this period of record occurred in June or the last week of May, with two exceptions. An annual peak discharge of 28.9 $m^3 s^{-1}$ occurred on July 9, 2011, and an annual peak discharge of 32 $m^3 s^{-1}$ occurred on September 12, 2013, during the 2013 extreme precipitation event.

2.4. Channel Morphology and OC Retention in the CFR

Past work suggests that valley geometry largely controls sediment storage in floodplains within the study area. The geomorphic impact of the 2013 floods in the CFR suggested that valley confinement and overbank stream power, which were significantly lower in glaciated valleys, were among the strongest predictors for floodplain sediment residence times (Sutfin & Wohl, 2019). Unconfined glaciated valleys attenuate flood waves by allowing flows to spread across the floodplain, which dissipates energy and decreases both the flow velocity and sediment transport capacity. Sediment residence times were also significantly shorter in the montane zone than in the subalpine zone (Sutfin & Wohl, 2019), both of which are characterized by distinctly different forest types and fire regimes (see Section 2.2).

Channel morphology and OC retention in the CFR are also influenced by large wood (>10 cm in diameter and >1 m in length) and logjams. Streams in the CFR are dominated by cobble to boulder substrate and typically maintain plane bed to step-pool morphologies, but transitional morphological states in channel form occur in response to altered wood regimes and reduced logjam occurrence (Livers et al., 2018). Instream wood loads and spacing of channel-spanning logjams are regulated by variability in forest age and valley geometry (Wohl & Cadol, 2011). Although large wood is a substantial component of OC storage in fluvial corridors of the CFR, logjams also facilitate OM retention (Beckman & Wohl, 2014). Prior work suggested that logjam-forced multithread channels increased OC storage per area in the CFR (Wohl et al., 2012), but that prior study was based on a limited number of study sites. In quantifying OC storage in floodplains of the CFR and identifying potential drivers of differences among channel and valley types, we examine whether and why logjam-induced multithread channels store more OC per area than other channel types.

3. Methods

In the following subsections, we describe several data sets and analyses including field observations, sample collection and analysis, GIS analysis, and statistical modeling to ask, "How do valley and channel morphologies influence floodplain OC storage in the Colorado Front Range?." To quantify differences in OC storage per area at 24 study reaches, we describe below methods for evaluating valley and channel morphology, surveying floodplain topography and sediment depth, calculating sediment volume (GIS), collecting litter and soil samples, surveying large wood on the floodplain, analyzing OC content, and quantifying OC storage along diverse channel types (Sections 3.1–3.5). To identify potential hydrogeomorphic mechanisms for differences in OC storage along valley segments with varying channel and valley geometry, we also present 6 years of logjam absence/presence surveys within a watershed encompassing nine of the 24 study reaches (Section 3.6). Two of the 24 study reaches were selected as intensive study sites and extended in length to include additional upstream and downstream reaches. Floodplain sediment and surface water samples were collected for detailed analysis of OM composition at the two intensive study sites to examine the role of channel morphology on OC molecular diversity and fate (Section 3.7). A salt tracer application was

conducted to calculate discharge within each study reach of the two intensive study sites during the time of sample collection (Section 3.8).

3.1. Study Reach Selection

We characterize study reaches by relative channel complexity and degree of valley confinement. We classify study reaches as abandoned or active beaver meadows based on field evidence of exposed or buried beaver dams and ponds, beaver-dug canals, beaver lodges, beaver mounds and slides, and beaver chewed trees (Ives, 1942; Polvi & Wohl, 2012, 2013). Within the CFR, old-growth forests (>200 years old) include trees that are large enough to create persistent channel-spanning logjams. Where logjams persist for a year or more, diversion of flows can form secondary channels and sometimes multiple channels of flow across relatively unconfined valley bottoms. We refer to these complex channel segments that lack evidence of beaver activity as multithread channels.

Stream reaches that are not multithread and lack evidence of beaver activity are classified using a valley confinement ratio (C_r), calculated as the stream channel width divided by the valley width. Stream reaches bounded entirely by bedrock and with the absence of a floodplain were considered extremely confined and were not included in the study. Reaches with $C_r > 0.5$ are classified as confined because a valley less than two times the width of the channel does not have space to accommodate channel avulsions or side channel development. Those with a ratio between 0.5 and 0.24 are defined as partly confined because overbank channels can be observed in these valleys, but multithread channels do not occur. Valleys with $C_r < 0.24$ are defined as unconfined valleys because these valleys accommodate the development of side channels, channel avulsions, and multithread channel systems.

This classification system results in five valley reach types including three classes in relatively unconfined valleys (beaver meadows, multithread channels, and unconfined reaches) and two classes in relatively narrow valleys (partly confined and confined reaches) (Table 1).

3.2. Field Surveys and Soil Sampling for OC Storage

We surveyed channel and valley geometry and measured the depth of floodplain fine sediment (summer 2012, 2013, 2014) along each of the 24 study reaches. Study reaches were defined by 11 surveyed transects spaced approximately one-bankfull width apart and oriented orthogonally to the down-valley direction. A stadia rod and a laser rangefinder with 10-cm accuracy (Laser Technologies®, TruPulse 360B) were used to survey topography along each transect at breaks in slope and other points of interest (e.g., changes in grain size, transitions in vegetation type) with a maximum spacing of 11 m between survey points. The depth of the underlying floodplain fine sediment (<2 mm) was measured at each survey point by inserting a 1-cm diameter soil probe into the floodplain surface. The probe was pounded into the surface using a 1.4-kg sledgehammer until refusal at bedrock or coarser pebble and cobble material. Dominant vegetation (e.g., grasses, willows, tree cover) and primary tree types (e.g., blue spruce, aspen, subalpine fir) were noted at survey points along each transect to verify typical vegetation type but were not used in statistical models. Approximate bankfull channel width was determined between points along each transect using the height of depositional features that included point bars and changes in vegetation as primary bankfull indicators. The stream gradient was measured using a survey of the estimated bankfull stage on the banks along the length of each study reach. Contributing drainage area for each study reach was calculated using 10-m resolution USGS digital elevation models (DEMs) in ESRI ArcMap. The elevation of each reach was taken as the elevation from the DEMs at the downstream transect along each study reach. Stream gradient was calculated as the slope of the linear regression line fit to all surveyed stream gradient points described above.

Soil sample locations were selected by systematic random sampling along each transect (Figure S1). Bootstrap analysis indicated that the variance and bias of the estimated mean OC content (for the entire depth of the sediment sampled at 15-cm increments) declined rapidly with an incremental increase in sample size until it leveled off at 11 sampling locations (Sutfin & Wohl, 2017). Bias was not further reduced until >30 sampling locations were included. We used these findings as guidance, and randomly selected a single sampling location along each of the 11 transects at each study reach to examine variability in OC content. The distance of each transect across the valley bottom was measured and potential sample locations were

Table 1
Physical Attributes of the 24 Study Reaches

Reach	Stream	Valley type	Mean valley width (m)	Mean channel width (m)	Mean valley confinement (m/m)	Mean gravimetric soil moisture content (%)	Stream gradient (m/m)	Elevation (m)	Drainage area (km^2)
1	NSV	Confined	18	13.0	0.73	16	0.032	2,385	97.7
2	Ouzel	Confined	9	5.3	0.55	35	0.095	2,971	10.7
3	GCK	Confined	12	8.5	0.32	34	0.13	2,845	21.0
4	NSV	Confined	11	6.2	0.58	38	0.085	2,951	17.9
5	NSV	Confined	19	14.1	0.74	20	0.026	2,162	205.1
6	GCK	Confined	10	5.6	0.50	42	0.09	3,071	9.7
7	NSV	Partly confined	33	17.1	0.45	21	0.037	2,420	96.4
8	Ouzel	Partly confined	14	5.1	0.34	38	0.063	2,927	11.1
9	GCK	Partly confined	33	8.5	0.26	25	0.027	2,701	33.2
10	Hunters	Partly confined	15	3.7	0.24	30	0.069	3,013	10.1
11	NSV	Partly confined	27	12.7	0.45	23	0.023	2,226	200.5
12	GCK	Partly confined	14	4.2	0.28	34	0.02	3,118	7.1
13	NSV	Partly confined	43	14.5	0.31	48	0.016	2,573	77.4
14	Cony	Unconfined	26	5.6	0.21	58	0.028	3,054	12.7
15	GCK	Unconfined	32	5.1	0.15	54	0.013	3,053	10.3
16	Mills	Unconfined	47	7.8	0.10	41	0.01	2,797	3.0
17	NSV	Beaver	67	6.8	0.10	55	0.037	2,901	19.1
18	Ouzel	Beaver	43	7.0	0.13	65	0.04	2,978	10.6
19	NSV	Beaver	247	14.1	0.05	40	0.012	2,547	82.2
20	BTR	Beaver	180	17.3	0.09	29	0.006	2,462	93.7
21	SFP	Beaver	77	10.6	0.13	25	0.011	2,410	180.6
22	NSV	Multithread	61	6.5	0.10	44	0.063	3,035	14.8
23	GCK	Multithread	34	6.7	0.18	39	0.03	3,068	9.8
24	Ouzel	Multithread	53	5.2	0.10	53	0.033	2,990	10.5

Note. Reach abbreviations include BTR = Big Thompson River, GCK = Glacier Creek, NSV = North Saint Vrain Creek, SFP = South Fork Cache La Poudre River.

represented by 1-m increments that spanned the distance along the transect. A random number generator was used to select a distance from the valley edge for each sample location. Locations falling within the active channel were shifted to the first meter on the left or right riverbank by random selection. Locations that fell on bedrock resulted in a new random selection without replacement. When only bedrock was present along cross sections, no sediment samples were collected, although litter and duff were collected if present.

A 7-cm diameter cylindrical sampling tube was used to collect a single volumetric sample of OM in the O-horizon at each sampling location. A 7-cm diameter stainless steel hand auger was used to sample fine sediment at increments of 15-cm depth until refusal at bedrock or clasts that exceeded ~2 mm in diameter. Auger length prevented sample collection at depths greater than 180 cm, which occurred at three sampling locations. In total, 660 sediment samples were collected at 273 sampling locations.

A total of 21 volumetric soil samples were collected in small pits excavated along the floodplain to estimate bulk density. A 7-cm diameter soil sampling tube was inserted horizontally and centered at ~5, 15, and 45-cm depth, where roots did not interrupt sampling (Supplemental Table S1).

3.3. Analysis of OC Content

Mineral soil samples were collected from the 24 study reaches and frozen until analysis for OC content by the Colorado State University Soil and Water Testing Laboratory. An aliquot of each sample was dried for 48 h at 60°C, then ground and analyzed for total C and N by dry combustion (LECO 1000 CHN analyzer, LECO Corporation, St. Joseph, MI, USA). To determine inorganic carbon concentrations (CO_3-C), each sample was treated with 0.4 N HCl and the CO_2 loss was measured gravimetrically. Soil OC content was calculated as total carbon minus CO_3-C. The gravimetric soil moisture content was determined as the difference between the mass of field-moist soil before and after it was dried at 105°C for 24 h.

A total of 281 O-horizon samples were processed for OC content. Recognizable plant material (<6 mm diameter, including litter and needles) and duff (unrecognizable and fragmented material between the litter and mineral soil layers; FIA, 2019) were dried at 105°C for 24 h. The OC content of the combined O-horizon (litter + duff, hereafter referred to as "litter") was determined using the loss on ignition method and estimated as 50% of the mass lost after 24 h at 550°C.

3.4. Organic Carbon Storage as Floodplain Large Wood

Wood surveys were conducted across the entire floodplain surface at each of the 24 study reaches to estimate OC storage in large wood. The length and diameter of all floodplain wood (greater than 1 m in length and 10 cm in diameter) were measured and wood volumes were calculated as the volume of a cylinder using the average diameter of the two-end measurements. The mass of C stored in each large wood piece was estimated using a calculated average density for species in the study area (Douglas fir, lodgepole pine, ponderosa pine, Engelmann spruce, and aspen) of 400 kg m^{-3} (Glass & Zelinka, 2004) and assuming 50% C by mass.

3.5. Organic Carbon Storage Per Area in Wood, Litter, and Sediment

Total OC storage was calculated in three compartments (i.e., sediment, wood, and litter) for each of the 24 study reaches and presented as the mass of OC per floodplain area.

Given the heterogeneity of floodplain erosion and sedimentation, it is possible that organic-rich layers of sediment lie beneath lenses of gravel at some study sites, which could result in underestimates of OC storage in our analysis. Heterogeneity of floodplain architecture results in poorly defined soil profiles and isolated buried lenses of organic-rich sediment that appeared to typically be ~1–3 m in length. Interpolating these high OC content values between transects would assume that those organic-rich layers span distances of over 50 m in length in some cases. We calculated depth-averaged OC content of systematic randomly sampled sediment, which incorporates these high values of OC content into estimates of storage without assuming unrealistic extent of those organic-rich lenses. While there is potential that our surveys did not capture some lenses of fine sediment and OM buried by gravel, we assume that the stress necessary to transport gravel is likely to erode finer sediment and OM present on the floodplain prior to the deposition of gravel.

The mass of OC stored in fine sediment at each study reach was estimated using soil samples, depth measurements, and GIS. The volume of floodplain fine sediment was calculated using measured depths of fine sediment and triangular irregular networks (TINs) in ESRI ArcMap. Sediment volumes were multiplied by the average bulk density across study reaches ($\rho_b = 0.9 \pm 0.24$ g cm^{-3}, Table S1), to estimate the mass of floodplain fine sediment along each study reach. The total mass of fine sediment along each study reach was multiplied by the mean gravimetric OC content along each reach to calculate the total mass of OC storage in floodplain sediment.

The mass of OC storage as litter was estimated using an average litter depth, OC content, and bulk density. The average depth of the litter layer was multiplied by the floodplain surface area, generated from TINs as described above, to estimate O-horizon volumes in each reach. Litter mass (calculated as the average bulk density multiplied by the volume of litter) was multiplied by the average OC content to estimate the mass of OC storage in litter for each reach.

The total mass of OC in all floodplain reservoirs (i.e., wood, sediment, litter) was divided by the surface area of each TIN to estimate total OC storage per area along each study reach.

3.6. Instream Logjam Surveys and Fine Sediment Depth

We utilized an ongoing presence-absence survey of logjams in the NSV watershed to examine relationships between logjams and the depth of floodplain fine sediment at nine of the 24 study reaches. The number of instream logjams was monitored and recorded annually over a 6-year period from 2010 to 2015 (Table S2). Locations of logjams upstream of the Pleistocene terminal moraine, located at ~2,500 m elevation, were recorded using a handheld GPS unit. Logjams that fell within the ESRI ArcMap shapefile extent of the surveyed study reach, plus one channel width up and downvalley of each study reach, were counted for each year. We estimated mean floodplain fine sediment depth by dividing the floodplain sediment volume described in Section 3.5 by the TIN surface area of the study reach. Because floodplain fine sediment depth among study reaches was significantly different between confined and unconfined reaches ($p < 0.05$), we accounted for varying degrees of confinement by standardizing sediment depth by the mean valley width. Using stepwise linear regression, we examined the influence of potential predictor variables (e.g., 6-year average number of logjams, drainage area, elevation, stream gradient) on floodplain fine sediment depth.

3.7. Analysis of Stream and Soil Water Chemistry

Additional surface water and soil samples were collected at the two intensive study sites that captured channel transitions (single-multiple-single thread) on Ouzel and GCK (August 18 and 19, 2014). We used these channel transitions to examine relative changes in dissolved OM composition upstream and downstream of the multithread reaches. The Ouzel Creek intensive study site was ~1,330 m long, with an upstream confined reach of 180 m, a middle multithread reach of 800 m, and a lower confined reach of 350 m in length. The GCK intensive study site was ~220 m long, with an upper confined reach of 65 m, a middle multithread reach of 90 m, and a lower partly confined reach 65 m in length. Transects were located near both the upstream and downstream extent of each of the three reaches, which resulted in six transects that defined each of the two intensive study sites. Soil core sample locations were selected on both channel banks of each transect and an island along each multithread transect using the same random selection process described in Section 3.2. Litter was removed, and fine mineral sediment was sampled where present (some locations were located on bedrock, boulders, or contained only litter) in increments of ~15 cm until refusal at bedrock or gravel. The number of soil samples collected at each site varied by the depth of available fine sediment/mineral soil, which was sometimes zero (Table S3). Surface-water samples were collected at one location along each of the confined transects and within the main stem and from at least one side channel along the multithread reaches (totaling eight samples for GCK and nine samples for Ouzel Creek). Acid-washed Nalgene® HDPE bottles were rinsed six times with water before a sample was collected. All samples were taken back to the lab; soil samples were frozen until further analysis and water samples were processed within 6 h.

We quantified dissolved organic carbon (DOC) concentrations in surface-water samples and floodplain soils and fine sediments. Within 6 h of collection, lotic samples were filtered through precombusted (400°C) 0.7 μm glass fiber filters (Whatman GF/F) and acidified to pH 3. Floodplain soils were extracted by combining 5 g of soil with 10 mL of nanopure water (<18.2 MΩ cm) in sterile 50 mL centrifuge tubes fit with 0.45 μm spin filters. Samples were centrifuged for 20 min at 3,400 rpm and 24°C and supernatants were collected for analysis. DOC concentrations were determined by high-temperature combustion catalytic oxidation using a Shimadzu TOC-V_{CPN} analyzer equipped with a sparging method for nonpurgeable OC (Shimadzu Corporation Columbia). Instrument detection limits were 50 μg DOC L^{-1}.

We assessed the structural properties (related to DOM source and bioavailability) of UV-fluorescent dissolved organic matter (FDOM) in surface water and floodplain soil water leachates using an Aqualog spectrofluorometer equipped with a xenon excitation source (Horiba-Jobin Yvone Scientific Edison). Filtered surface and floodplain water extracts were normalized to 5 mg C $L^{-1,}$ to reduce inner-filter effects. Excitation emission matrices (EEMs) fluorescence scans were completed from 240 to 600 nm excitation and emission wavelengths, with 3 nm bandpass, 3 nm increments, and 3 s integrations. A sealed cuvette of deionized (DI) water was analyzed between every 10 samples to account for instrument drift and minimize the influence of water Raman peaks in sample spectra. Scans were blank corrected using DI water and corrected for inner filter effects (Kubista et al., 1994). First- and second-order Raleigh scattering were masked (10 nm width masking), and samples were normalized by the area of the DI water Raman scattering peak (Lawaetz & Stedmon, 2009).

We quantified five spectral FDOM regions to assess the complexity and heterogeneity of surface-water and floodplain soil leachates using the fluorescence regional integration (FRI) approach (Matlab R2016b) as outlined by Chen et al. (2003). Because the FRI approach quantifies regions of wavelength-dependent fluorescent intensities, it is well suited to capture the underlying heterogeneity and compositional quality of DOM leached from floodplain soils (Lynch, Sutfin, et al., 2019). EEMS regions I and II are related to simple proteins (with similar fluorescence characteristics as tyrosine and tryptophan). Region III is related to lower molecular weight, aromatic compounds similar to fulvic acids. Region IV resembles soluble microbial byproducts, and region V is linked with polyaromatic compounds similar to lignin derivatives, tannins, and polyphenols (Chen et al., 2003; Fellman et al., 2010). Ultraviolet absorbance at the 25 nm wavelength was divided by DOC concentration to calculate $SUVA_{254}$ (L mg C^{-1} m^{-1}), an indicator of FDOM aromaticity or complexity (Weishaar et al., 2003).

3.8. Tracer Application and Measurements of Discharge

Salt tracer applications were used to estimate stream discharge at each intensive study site on the day of sampling for surface water and soils used in fluorescence analysis (see Section 3.7). After surface water and soil sample collection was completed, stream tracer additions of NaCl were added as a single pulse to the upstream end of the upper confined study reach for the Ouzel Creek (10,000 g) and GCK (6,000 g) intensive study sites. Downstream changes in specific conductivity were monitored (3-s logging interval, Hobo Conductivity Logger; Onset, Bourne, Massachusetts) at the downstream end of the upper confined reach. Conductivity sensors were removed after conductivity reached background conditions. The total specific conductivity from the tracer application was calculated by integrating beneath the specific conductivity curve. The tracer applications were used to calculate discharge (Q) flowing into each of the two intensive study sites as

$$Q = \frac{SC_{\text{added}}}{\sum_{i=1}^{n}\left(SC_{\text{meas}}\ x\ \Delta t\right)} \tag{1}$$

where SC_{added} was the specific conductivity of the NaCl added at the upstream end of each intensive study site, and Δt was the duration of each time step (3 s). SC_{meas} was the specific conductivity measured at the downstream end of each reach and corrected for ambient conductivity. NaCl tracer additions were conducted as part of an unpublished $NaNO_3$ uptake study. Additional details and appropriate corrections associated with these salt applications are provided in supporting information.

3.9. Statistical Analysis

Statistical analyses included examination of correlations, pairwise comparisons, transformations, and stepwise linear regression, all of which were conducted using R statistical software (R Core Team, 2017).

Differences in OC storage per area within wood, sediment, and litter (and the sum of all three reservoirs) between valley types were tested using Tukey honestly significant difference (HSD) pairwise comparisons. For these comparisons, storage in large wood, soil OC, and the sum of all three reservoirs required log transformation to meet assumptions of normality and homoscedasticity. OC storage in litter required no transformation.

We reduced variable redundancy in regression analyses by eliminating independent variables that were strongly cross-correlated, or inherently linked, with other variables (Tables S4 and S5). To examine factors that controlled OC storage per area and the depth of floodplain fine sediment, potential predictor variables were selected using the following systematic process: the predictor most strongly correlated with the outcome variable was selected as the first predictor and all other variables highly correlated ($r > 7$) with any previously selected variables were eliminated.

Once variable selection was completed, exhaustive (backward and forward) stepwise multiple linear regression was conducted to determine the model that best explained the outcome variable as indicated by the minimized Akaike Information Criterion (AIC; Akaike, 1998). OC storage per area was transformed with a boxcox power transformation (to meet the assumptions of normality and homoscedasticity) to identify

variables that influenced the combined OC storage in all three reservoirs (i.e., wood, sediment, litter). No transformations were needed to meet regression assumptions when predicting fine sediment depth normalized by valley width (stepwise linear regression metrics, transformations, and results are listed in Table 3). We evaluated normality of model residuals with Shapiro-Wilk tests (shapiro.test in R) and examination of qq-plots and histograms. Homoscedasticity was verified by failing to reject the null hypothesis with an alpha level of 0.05 for the studentized Breusch-Pegan test (bptest function in R).

Principle components analysis (PCA) was conducted on EEMS indices to examine differences in the chemical composition of OC in surface waters and floodplain leachates collected along intensive single-multiple-single thread intensive study reaches.

4. Results

We find that OC storage is greatest in reaches with deep floodplain sediments, particularly within unconfined single-thread channels. Our results also indicate that logjams play a substantial role in reducing soil OC storage in multithread stream reaches. The strongest predictors of sediment depth included channel slope, valley confinement, and the number of logjams (6 year average). Relative to unconfined single-thread channels, multithread stream reaches had shallower sediments, lower mean OC contents, and evidence of increased microbial activity and OM transformation.

The following subsections summarize (a) OC storage per area in three reservoirs (wood, sediment, and litter), focusing on differences in OC storage by valley and channel type (24 study reaches), (b) the role of logjams and channel geometry on floodplain sediment depth (subset of 9 study reaches), and (c) downstream shifts in FDOM composition through transitions in channel complexity in logjam-induced multithread reaches (two intensive study sites).

4.1. Organic Carbon Storage by Valley Type in Wood, Litter, and Sediment

Floodplain OC storage in the study area was dominated by the fine sediment component (102 ± 35 to 464 ± 165 Mg C ha^{-1}) for all channel types, but relative amounts of storage in all reservoirs differed across valley and channel type (Figure 2). Unconfined single-thread reaches stored more OC in fine sediment (464 ± 165 Mg C ha^{-1}) than beaver meadows (276 ± 179 Mg C ha^{-1}) and significantly more than confined and partly confined reaches (Table S6). Among all the study reaches, large floodplain wood loads (13 ± 23 to 42 ± 3 Mg C ha^{-1}) were the smallest reservoir for OC storage (Table S6), followed closely by litter (20 ± 12 to 40 ± 7 Mg C ha^{-1}). Among all channel types, beaver meadows contained the lowest OC storage as large floodplain wood and litter (13 ± 23 Mg C ha^{-1}) and multithread channels stored the most (42 ± 3 Mg C ha^{-1}). Higher OC storage in wood and litter within multithread reaches, relative to beaver meadows and unconfined single-thread streams, reflects the abundance of old-growth conifer trees in multithread reaches and the limited number of trees in grass-dominated and willow-dominated meadows.

Unconfined valleys (unconfined single-thread, beaver meadow, and multithread reaches) stored more OC (346 ± 177 Mg C ha^{-1}) per area in all reservoirs compared to more narrow valleys (confined and partly confined reaches; 188 ± 107 Mg C ha^{-1}) (Figure 2, Table S6). Unconfined single-thread reaches stored significantly more OC in all combined reservoirs than confined reaches (Figure 2). Within unconfined valleys, OC storage differed across reach type depending on channel complexity (i.e., beaver meadows, multithread, unconfined single-thread reaches). Unconfined single-thread channels (502 ± 161 Mg C ha^{-1}) stored more OC per area than more complex beaver meadows (309 ± 195 Mg C ha^{-1}) and multithread reaches (252 ± 39 Mg C ha^{-1}) (Figure 2, Table 2).

Stepwise regression results indicate that OC storage per area is greatest in less confined valleys, low-gradient streams, and at higher elevations. The optimal regression model explaining potential controls on the amount of OC storage per area includes elevation, stream gradient, and valley confinement (Table 3). This makes sense because narrow valley types (confined and partly confined reaches) that store less OC per area have steeper stream gradients and are more confined. Valley confinement also increases below the terminal extent of Pleistocene glaciation and the knickpoint at the contact between igneous and sedimentary rocks.

Table 2
Floodplain organic Carbon Storage in Litter, Large Wood, and Soil + Fine Sediment Among all Study Reaches

				Wood		Litter and humus		Soil and sediment				Combined
Reach	Stream	Valley type	Valley area (ha)	Volume (m^3)	Carbon storage (Mg C ha^{-1})	Volume (m^3)	Carbon storage (Mg C ha^{-1})	Mean SOC (%)	Mean depth (m)	Volume (m^3)	Carbon storage (Mg C ha^{-1})	Carbon storage (Mg C ha^{-1})
1	NSV	Confined	0.09	16.8	36.5	82.4	61.0	3.0	0.25	229.8	67.7	165.3
2	Ouzel	Confined	0.02	6.6	61.7	19.3	37.6	6.6	0.22	47.3	130.8	230.1
3	Glacier	Confined	0.01	0.6	14.1	7.3	33.5	14.4	0.09	7.9	112.3	159.8
4	NSV	Confined	0.03	2.1	14.7	26.1	31.8	9.7	0.15	41.4	128.8	175.3
5	NSV	Confined	0.04	0.8	3.8	18.0	13.7	2.6	0.21	90.3	50.5	68.0
6	Glacier	Confined	0.04	0.9	4.6	27.6	32.0	8.7	0.16	59.4	124.5	161.1
7	NSV	Partly confined	0.30	17.5	11.5	209.9	37.7	4.4	0.19	590.0	76.7	126.0
8	Ouzel	Partly confined	0.06	15.8	55.5	47.4	35.0	9.2	0.18	100.6	146.3	236.8
9	Glacier	Partly confined	0.26	28.2	21.4	200.3	35.1	4.0	0.19	509.2	70.2	126.7
10	Hunters	Partly confined	0.05	10.7	42.2	40.0	37.5	3.2	0.33	169.1	96.9	176.7
11	NSV	Partly confined	0.26	3.5	2.7	51.8	17.7	3.0	0.32	815.6	85.0	105.4
12	Glacier	Partly confined	0.05	1.1	4.7	14.4	9.1	13.2	0.42	193.0	492.8	506.6
13	NSV	Partly confined	0.43	17.7	8.3	299.6	53.6	3.4	0.46	1,966.3	139.0	200.8
14	Cony	Unconfined	0.13	18.4	27.8	47.1	24.4	19.0	0.30	402.4	516.9	569.1
15	Glacier	Unconfined	0.15	5.0	6.7	80.1	16.0	13.5	0.49	729.5	595.7	618.5
16	Mills	Unconfined	0.21	7.4	7.1	173.6	32.4	5.4	0.57	1,186.3	279.1	318.6
17	NSV	Beaver	0.58	23.0	7.9	546.1	32.1	11.6	0.54	3,126.2	565.1	605.2
18	Ouzel	Beaver	0.30	79.5	53.4	265.5	30.4	12.5	0.26	773.7	292.5	376.3
19	NSV	Beaver	5.04	14.7	0.6	2,109.6	20.3	5.2	0.57	28,798.5	266.3	287.2
20	BTR	Beaver	3.27	16.4	1.0	1,090.6	12.1	2.3	0.60	19,501.1	124.0	137.2
21	SFP	Beaver	0.81	14.6	3.6	91.5	3.1	2.8	0.51	4,187.5	130.4	137.1
22	NSV	Multithread	0.49	103.1	42.0	558.5	43.5	5.2	0.26	1,269.3	121.5	207.0
23	Glacier	Multithread	0.12	26.8	45.5	106.0	31.7	9.6	0.23	268.6	196.9	274.1
24	Ouzel	Multithread	0.37	74.1	39.9	452.4	44.5	8.9	0.24	881.7	190.7	275.1

Note. Stream abbreviations include BTR = Big Thompson River, GCK = Glacier Creek, NSV = North Saint Vrain Creek, SFP = South Fork Cache La Poudre River.

Unconfined single-thread and beaver meadow reaches are less confined and tend to have lower stream gradients than multithread reaches and narrower valley types (Table 1).

Differences in OC storage among the three unconfined valley types (beaver meadows, multithread, and unconfined single-thread reaches) are reflected in sediment depth and OC content. Beaver meadows and unconfined single-thread channels have higher mean floodplain fine sediment depth than multithread channel reaches, although these differences are not statistically significant (Figure 3a). Unconfined single-thread study reaches also have the highest mean OC content across all channel types and substantially more than multithread channel reaches (Figure 3b).

4.2. Logjams and Fine Sediment Storage

The optimal model from stepwise multiple linear regression indicates that ~74% of the variability in average floodplain fine sediment depths, standardized by valley width, is best explained by the 6-year average number of logjams ($p < 0.05$), stream gradient ($p < 0.05$), drainage area, and elevation (Table 3). The latter two variables were not statistically significant, although they were retained in the optimal regression

Table 3
Stepwise Regression Transformations, Variable Coefficients and Significance, and Results

	Combined OC storage		Fine sediment depth standardized by valley width	
Transformation	$\lambda = -0.38384$		n/a	
Intercept	3.49×10^{-01}	***	-9.11×10^{-02}	
Elevation	-8.17×10^{-05}	***	3.53×10^{-05}	
Stream gradient	3.34×10^{-01}	*	1.60×10^{-01}	*
Confinement	-1.11×10^{-03}		n/a	
Drainage area	n/a		-6.77×10^{-04}	
Annual average number of logjams	n/a		-2.40×10^{-03}	*
r^2	0.71	***	0.74	*
p-value	3.46×10^{-06}		0.05	

Note. Statistical significance for each variable and optimal multiple linear regression model denoted, with *** for $p < 0.001$, ** for $p < 0.01$, and * for $p < 0.05$. OC, organic carbon.

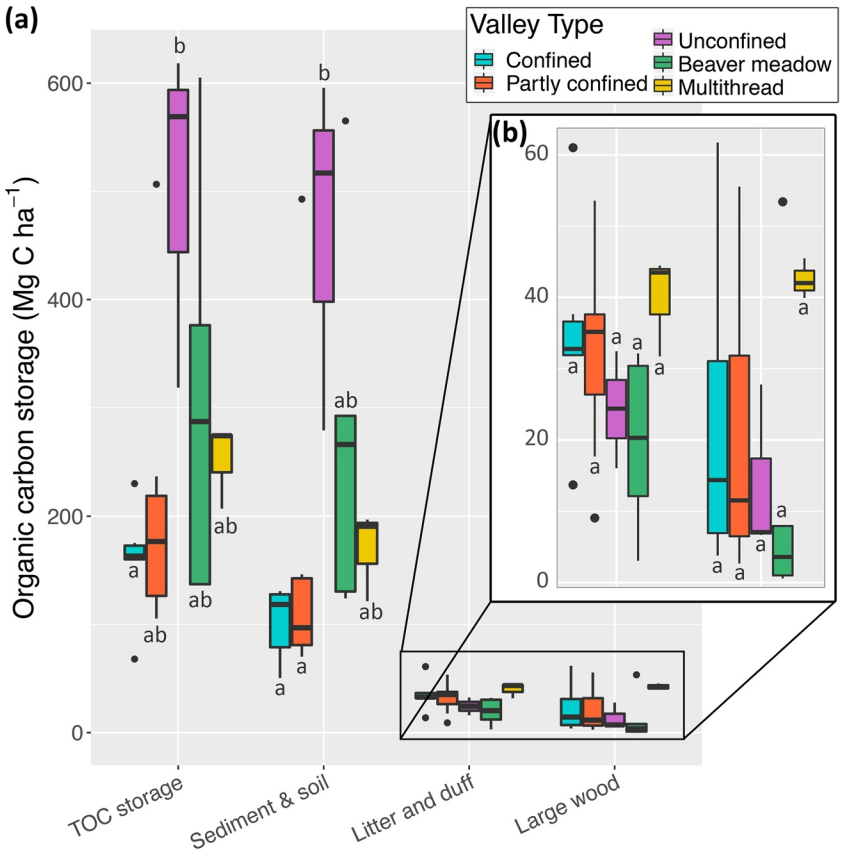

Figure 2. Box plots of organic carbon (OC) storage per area. The 24 study reaches are represented by five valley types that vary by degree of confinement and channel complexity. (a) TOC (total OC) is the sum of combined OC stored in (i) floodplain fine sediment and soil, (ii) litter, and (iii) large wood. (b) The zoomed in area of OC storage as wood and litter used a smaller scale to provide detailed differences between channel type. Letters *a* and *b* indicate group assignments for channel types within each OC reservoir (based on statistical significance at the 95% confidence level using Tukey HSD pairwise comparisons). Channel types sharing any combination of *a* or *b* are not significantly different, whereas channel types that do not share a common letter are significantly different.

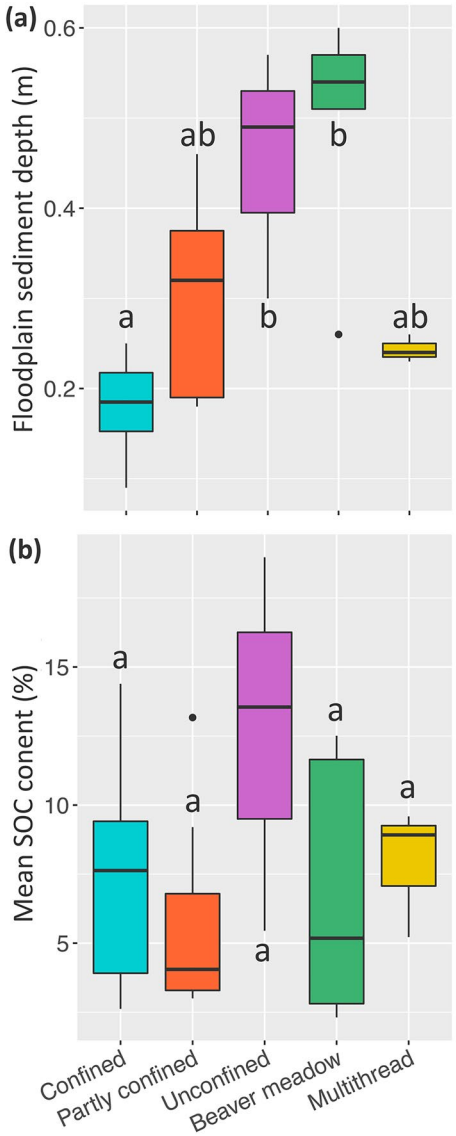

Figure 3. Boxplots of floodplain soil depth (a) and mean soil organic carbon (OC) content (b) by valley type. Letters *a* and *b* indicate group assignments for channel types within each OC reservoir (based on statistical significance at the 95% confidence level using Tukey honestly significant difference [HSD] pairwise comparisons). Channel types sharing any combination of *a* or *b* are not significantly different, whereas channel types that do not share a common letter are significantly different.

model ($p < 0.05$). This means that increased number and frequency of logjams within a given river segment is linked with shallower floodplain fine sediment when also considering valley width and stream gradient (Supplemental Table S5).

4.3. Organic Matter Composition in Multithread Intensive Study Reaches

Using principal components analysis (PCA), we identified relationships between channel complexity and the structural characteristics of fluorescing dissolved OM (FDOM) collected from stream flow and adjacent floodplain soils within the two intensive study segments. FDOM signatures of stream water samples indicate distinct changes in DOM composition at transitions from confined to multithread channels. Stream water (Figure 4a) flowing from confined reaches into multithread channel reaches had optical properties consistent with terrestrially derived organic acids (regions III and V). FDOM complexity ($SUVA_{254}$) and the relative abundance of protein-like compounds (EEMS regions I, II) that are typically associated with microbial sources increased within multithread networks. Regions II and V were also more variable within multithread reaches, potentially reflecting more diverse pathways for microbial transformation of terrestrially derived OC. Surface water flowing through lower confined reaches retained the heterogeneous signature imparted by multithread channels, with relatively more microbially derived proteinaceous features than upper confined reaches (Figure 4c).

EEMS spectra of floodplain soil leachate contained a similar, but opposite, shift in the signatures of FDOM compared to surface water at the study sites. The relative intensities of EEMS regions II and IV (representing simple proteins and byproducts of microbial metabolism) were highest in soil leachate collected from upper, confined reaches flowing into multithread channels (Figure 4b). Similar to the pattern found in surface waters, the fluorescent properties of floodplain soil leachates within multithread reaches reflected both terrestrial and microbially sourced OC. However, the variability in fluorescence spectra of floodplain leachates collected from multithread reaches was more constrained, relative to upstream and downstream single-thread reaches, than that found in adjacent surface waters (Figure 4b). Floodplain soil leachates collected from lower confined reaches had higher relative percent intensities of regions III and V, reflecting a more diverse array of terrestrially derived organic acids relative to the upstream reach. Overall, FDOM variability was highest in multithread reaches. Although FDOM variability decreased in single-thread reaches downstream of multithread reaches, structural complexity was retained within lower single-thread reaches relative to upper confined channels (Figure 4c).

Discharge during the time of sampling was typical of mean flows in August at the base of receding limbs of annual snowmelt-dominated hydrographs. Discharges measured from tracer additions at the intensive study sites were 0.27 $m^3\ s^{-1}$ at Ouzel Creek and 0.20 $m^3\ s^{-1}$ at Glacier Creek. We use relative comparison of discharge during typical years and the time of sampling at a USGS gauge ~8-km downstream from the Glacier study site to place our measured discharge values into context. Monthly average discharge at the Big Thompson Creek gauge at Moraine Park during June, July, August, and September are 7.37, 3.64, 1.38, and 0.86 $m^3\ s^{-1}$, respectively. For comparison, discharge at the BTR gauge downstream of the Glacier Creek intensive study site was 1.39 $m^3\ s^{-1}$ during the day of sampling, indicating average flow conditions in August (Figure S2).

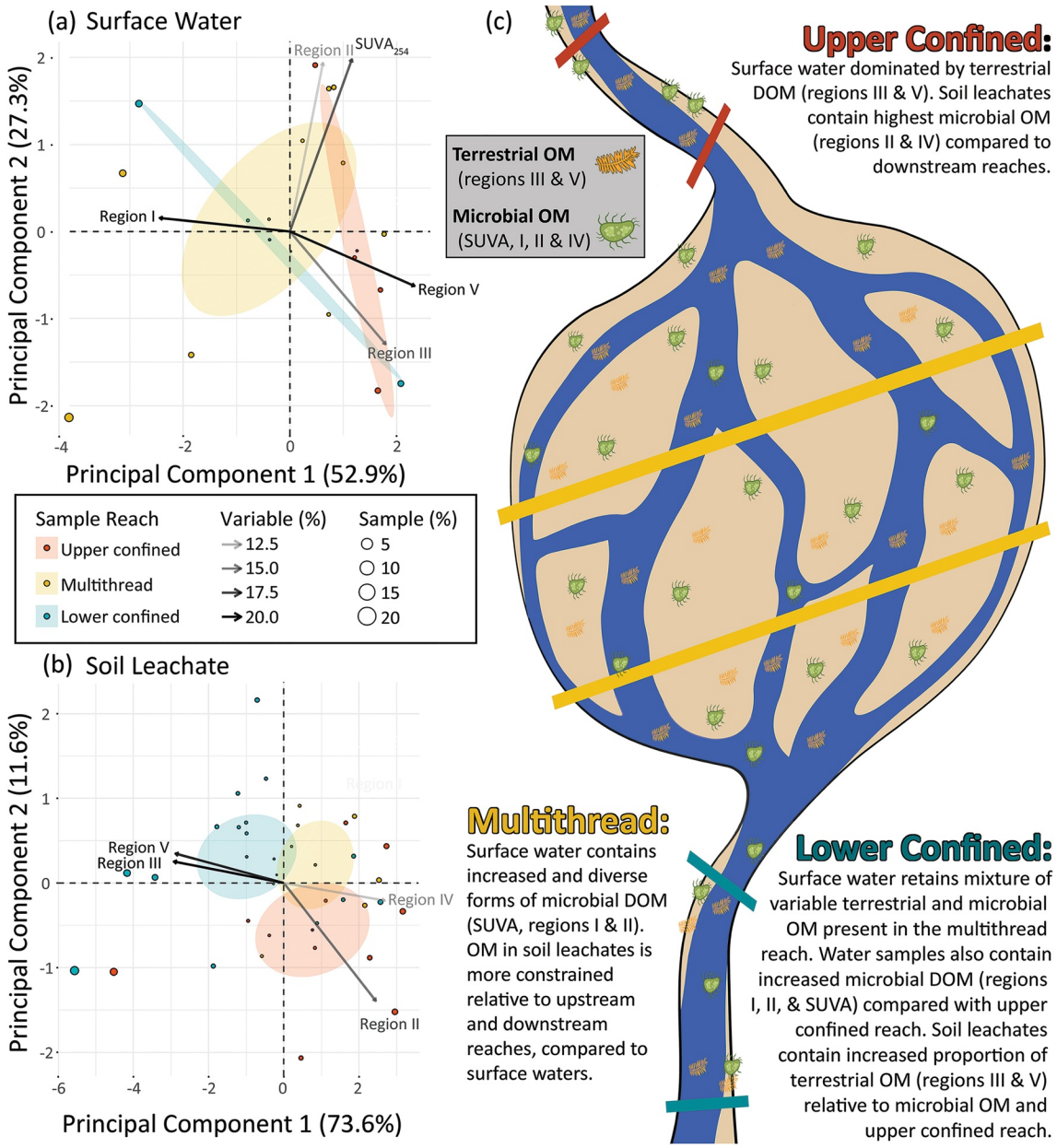

Figure 4. Principal components analysis (PCA) of fluorescent dissolved organic matter (FDOM) composition (a), (b) and a diagram illustrating results as a function of channel complexity (c). The contribution (in percent) of individual variables (vector shade) and samples (symbol size) to principal components 1 and 2 are shown for (a) surface waters and (b) soil leachates (data provided in Table S7). Shaded ellipses correspond to 95% confidence intervals for the upper confined (red), lower confined (blue), and middle multithread (yellow) reaches. The diagram (c) depicts two sampling transects within each reach (colors match PCA plots).

5. Discussion

5.1. Organic Carbon Storage by Valley Type and Valley-Channel Morphology

Our findings build upon previous work by showing that unconfined valleys store more OC per area than confined valleys (Wohl et al., 2012), but also elucidate mechanisms to explain why OC storage per area is not highest in logjam-induced multithread channels or beaver meadows.

Although OC storage in beaver meadows was lower than unconfined single-thread channels, beaver meadows do constitute substantial storage. While similar levels of OC storage in Colorado Front Range (CFR)

beaver meadows has been reported, OC storage appears to decrease when meadows are abandoned (Laurel & Wohl, 2019; Wohl, 2013a). Following beaver abandonment, channels incise and water tables decline, which likely reduces fluvial deposition of OM across the floodplain, increases mineralization of soil OC, and decreases riparian vegetation and associated litter inputs. All but one of the beaver meadows in our study were abandoned. Even when a beaver meadow is actively occupied, continual shifts in the connectivity of secondary channels and filled or drained ponds can cause local erosion of fine sediment and OM, as well as local fluctuations between saturated and reducing conditions. We infer that these factors limit soil OC storage relative to the continuously saturated soils observed at our unconfined single-thread stream sites.

Seasonal changes in hydrologic connectivity have also been correlated with shifts in the molecular composition of OM flowing through multithread beaver meadows (Lynch et al., 2019b). During base-flow conditions, Lynch et al. (2019b) found that DOM diversity increased as hydrologic connectivity declined. The authors attributed these observations to hydrologic fragmentation and greater turnover and release of microbial metabolites. The results we present here suggest similar hydrologic controls catalyze OM transformation because fine-sediment OC content is lower and FDOM signatures indicate greater microbial transformation of OM. Our results inform two conceptual models described in detail below that illustrate (a) observed decreases in fine sediment depth and (b) lower OC content along multithread reaches.

5.2. Logjams and Floodplain Fine Sediment Depth

Within unconfined valleys, the mean depth of floodplain fine sediment along single-thread channels (45 ± 14 cm) is deeper (although not significantly, $p = 0.3$) than multithread channels (24 ± 2 cm; Figure 3). As a result, fine sediment volume and OC storage per area are higher in unconfined single-thread reaches than multithread reaches despite similar valley widths.

Recruitment of old-growth trees into the stream channel and the formation of channel-spanning logjams can facilitate floodplain aggradation and complex topography in headwater streams (Sear et al., 2010). In large alluvial valleys, persistent logjams can also stabilize vegetated islands and promote floodplain fine sediment storage (Collins et al., 2012). However, our results along smaller streams (<200 km^2) suggest multiple channels of flow across the valley bottom limit total fine sediment storage for valleys of similar width.

Large instream wood and logjams act in tandem to separate flow, decreasing flow depth and shear stress available to transport sediment. Because large wood and logjams obstruct flow in channels, they dissipate force acting on the bed and partition shear stress so that less shear stress is available to transport sediment (Manga & Kirchner, 2000). The accumulation of gravel behind logjams (Cadol & Wohl, 2011) further diverts flow into multiple channels and could in turn contribute to the positive feedback involving bank erosion, tree undercutting, logjam formation, and channel avulsions (Polvi & Wohl, 2013; Sear et al., 2010). Transport of fine sediment within multiple channels of multithread reaches further limits fine sediment aggradation across the floodplain and vegetated bars (see extended discussion in supplemental material).

In contrast, single-thread unconfined channel floodplains dominated by densely growing rushes, sedges, and woody shrubs stabilize channel banks and provide erosional resistance (Simon & Collison, 2002). Energy dissipation across the broad floodplains of single-thread channels results in fine overbank sediment accumulation, providing additional bank cohesion and erosion resistance. Transport of both fine and coarse sediment in the channel and aggradation of the floodplain maintains larger channel cross-sectional areas and the ability to convey larger flows. The resulting increase in potential bed shear stress ensures continued transport of coarse grains and a positive feedback that maintains a single-thread channel. Accumulation of floodplain fine sediment and release of OM from floodplain vegetation (i.e., plant litter and root inputs) may further increase OC storage per area in single-thread channels of unconfined valleys.

5.3. Multithread Channels as Hotspots for OM Transformation

Multithread reaches contain lower OC content in floodplain fine sediments than their single-thread counterparts flowing through unconfined valleys (Table 2). This result is linked to two primary factors: (a) differences in OC sources and (b) inferred differences in mixing and transit times of water and entrained OC within multithread and single-thread reaches.

Although we assume a substantial portion of OC inputs to floodplains in the CFR are fluvially transported, a portion of OC is derived from in situ production, which differs among sites (Scott & Wohl, 2018). Multithread reaches flow through shaded conifer forests that lack abundant understory vegetation. Our observations of the highest wood and litter storage in multithread channels, compared with other stream types, indicate that coarse particulate OM is a substantial source of floodplain OC in these systems. In contrast, unconfined single-thread reaches have abundant rush and sedge communities that likely release root exudates and litter directly to the floodplain. Thus, differences in riparian vegetation, which covary with channel morphology, may play a role in OC storage by influencing the availability of OM inputs. High OC concentrations at unconfined single-thread sites could be influenced by greater litter inputs from dense wetland vegetation and reducing conditions that slow microbial decomposition compared to multithread channel reaches.

Observations of year-round floodplain saturation (i.e., standing water not coming from overbank flows) at some of the single-thread unconfined reaches, such as sites on Cony and Glacier Creeks, also suggest that groundwater upwelling from the highly jointed bedrock in these reaches helps to maintain reducing conditions in floodplain soils. Higher moisture content observed on the floodplain surface of unconfined single-thread floodplains compared to multithread reaches likely facilitates positive feedbacks with bedrock chemical weathering. Increased moisture at the bedrock/regolith interface increases chemical weathering and bedrock fracturing, which in turn could increase groundwater inputs into these reaches. Groundwater discharge could increase OC concentrations along unconfined floodplains, but organic-rich sedimentary rocks that could serve as sources of OC in groundwater are virtually nonexistent in the study area (Braddock & Cole, 1990). At the same time, high soil moisture within old-growth forest floodplains may limit (a) conifer growth, (b) wood recruitment to channels, (c) logjams, and (d) the transition into multithread channel systems, creating a stable state for moist, grassy floodplains.

Our observations of downstream shifts in FDOM composition within the Glacier and Ouzel Creeks intensive study sites provide mechanistic insight into the influence of channel complexity on OC cycling (Figure 4c). Surface water flowing through single-thread channels upstream of multithread systems had a higher relative abundance of FDOM compounds characteristic of terrestrial inputs (Figure 4a). Paired floodplain leachates reflected the signatures of microbial activity working to decompose that OM (Figure 4b). In contrast, FDOM pools in multithread channels had greater structural heterogeneity and a higher relative abundance of protein-rich microbial derivatives. FDOM signatures in downstream single-thread reaches reflect fluvial transport of complex terrestrial DOM from upstream multithread reaches. This lingering downstream increase in FDOM complexity may be caused by abundant hyporheic exchange, increased microbial transformation of OM, and OM flushing from floodplain sediments within multithread channel reaches.

Our findings reflect increased opportunities for terrestrially derived OM (e.g., lignin derivatives and higher molecular weight organic acids) to be compositionally altered by microbial transformation or photo-oxidation through abundant mixing and hyporheic exchange in multithread channels. Channel complexity increases hyporheic exchange, oxygen availability, and water and DOC transit times (Danczak et al., 2016; Gooseff et al., 2007). These conditions facilitate oxidation of OM (Battin et al., 2008; Boye et al., 2017), flushing of OM from floodplain sediment, and mixing of OM pools in both sediment and surface waters (Stegen et al., 2016, Figure 4c). Thus, microbial and invertebrate communities have greater opportunities to assimilate and transform OM, reducing OC storage through CO_2 mineralization to the atmosphere. These transformations have important implications for substrate quality as FDOM is exported to higher order river networks.

Findings presented here support past work that identified morphologically complex multithread streams as hotspots for the decomposition and transformation of OC (Battin et al., 2008; Lynch, Sutfin, et al., 2019). Complex channels in the CFR also support higher aquatic invertebrate and salmonid biomass relative to less complex, single-thread channels (Herdrich et al., 2018; Livers & Wohl, 2016; Venarsky et al., 2018; Wohl et al., 2017). Here, we show that increases in microbial activity and OM turnover within complex multithread reaches may provide the resources necessary at the bottom of the food web to facilitate greater productivity in these mountainous stream ecosystems.

6. Implications: Floodplain Organic Carbon Dynamics Under Shifting Hydrologic Regimes

Incorporating floodplain OC dynamics into the terrestrial C budget requires investigating potential changes in hydrologic flow regime, floodplain hydrologic connectivity, and erosion and aggradation dynamics that could alter sediment and OC floodplain reservoirs. The sensitivity of rivers to anticipated changes in precipitation and hydrologic flow regimes may shift the role of floodplains as OC sinks or sources (Lininger & Wohl, 2019; Sutfin et al., 2016). Observed decreases in snowpack, earlier snowmelt (Stewart, 2009), elevational shifts in rain-snow transitions (Kampf & Lefsky, 2016), and changes in precipitation regimes may drastically alter the timing, frequency, and magnitude of river flows (Bates et al., 2008).

Observed and projected changes in river flows in response to land use and flow regulation are well known (Dunne & Leopold, 1978; Poff et al., 1997; Richter et al., 1996), but those associated with climate change are riddled with uncertainty (Gudmundsson et al., 2019; Hirsch & Archfield, 2015; Sharma et al., 2018; Tabari, 2020). Responses to a changing climate and societal pressures (i.e., land use change, flow regulation) could alter floodplain OC storage within the CFR, similar snowmelt-dominated mountainous systems, and other rivers and streams subject to losses in channel complexity and hydrologic connectivity. We consider two possible contrasting, but not mutually exclusive, hydrologic responses that are influenced by climate and societal pressures: increase in floods and/or loss of hydrologic connectivity. Our results suggest river channel and valley geometry will modulate OC storage in floodplains.

Extreme precipitation may increase the magnitude of rare extreme floods (Gudmundsson et al., 2019; Tabari, 2020), which are exacerbated by deforestation (Dunne & Leopold, 1978), urbanization (Blum et al., 2020), and wildfire (Moody & Ebel, 2012), and alter floodplain aggradation, erosion, and OC storage. Within the CFR, steeper river channels in montane confined valleys are particularly susceptible to large floods (Sutfin & Wohl, 2019). Losses in floodplain sediment and associated OC storage were observed following the 2013 flood in the CFR (Rathburn et al., 2017), which evacuated floodplain fine sediment after sample collection occurred at four of our study reaches. Flood-enhanced bank erosion in confined reaches that recruits large wood to channels, combined with the high transport capacity of floods, also decreases the already low floodplain OC stock in the form of large wood in confined reaches.

In contrast, wider valleys have the capacity to accommodate floods, dissipate flow energy, and attenuate flood waves, all of which facilitate increases in fine sediment aggradation (Dunne & Leopold, 1978; Wohl et al., 2015), accumulation of large wood (Wohl, 2020), and greater OC storage (Sutfin et al., 2016). As a result, unconfined single-thread reaches have deeper fine sediment and higher OC content. In our study area, high elevation, unconfined valleys that are unaltered by wildfire in the last 500 years store sediment for more than 1,200 years (Sutfin & Wohl, 2019). We can, therefore, assume contemporary floodplain sediment represents sediment accumulation and storage over a range of annual floods upto approximately the 1,000 years flood. This indicates that single-thread and multithread streams in unconfined valleys will facilitate increases in sediment and OC storage during floods under both projected increases in extreme events (Gudmundsson et al., 2019; Tabari, 2020) and observed increases in the frequency of smaller floods (Hirsch & Archfield, 2015; Sharma et al., 2018). Our results suggest valley geometry will regulate OC accumulation across changes in flood frequency and magnitude, while channel complexity will regulate the mineralization of stored OC.

The 2013 flood did not significantly decrease channel and floodplain wood loads in subalpine unconfined reaches (Wohl & Scamardo, 2021), but the substantially larger sediment flux (partly influenced by valley-side landslides) and higher precipitation intensities did remove substantial quantities of large wood from the channel and floodplain in montane zone reaches of NSV (Rathburn et al., 2017). We do not know how far this wood might have moved downstream under natural conditions because a large reservoir immediately downstream from the study area trapped all of the mobilized wood. Thus, the influence of extreme floods on large wood reflects the influence of both valley geometry and elevational-dependent hydroclimatic regime.

Hydrologic connectivity across valley bottoms is anticipated to decline as a result of decreased snowpack, more frequent droughts, and lower baseflows (Alexander et al., 2015; Stewart, 2009). These effects may be most pronounced in unconfined valleys with varying degrees of channel complexity. For example, decreases

in lateral connectivity across valley bottoms limit overbank floodplain deposition and may reduce OC storage in single-thread valleys. In contrast, we anticipate a more complex response in multithread channel reaches, which support greater microbial activity and transformation of OM. Projected decreases in lateral and longitudinal hydrologic connectivity resulting from climate changes, flow diversions, and dams, will decrease local groundwater table elevations and rates of hyporheic exchange (Alexander et al., 2015). At our intensive study sites, samples were collected during relatively low flow conditions, which may explain observed increases in FDOM diversity within multithread reaches (Lynch, Sutfin, et al., 2019). The loss of hydrologic connectivity in multithread reaches that already exhibit lower OC content and greater microbial activity could facilitate a significant loss in soil OC storage and terrestrial sources of OM to downstream food webs. However, large wood recruitment to channels may increase under drier conditions as trees are stressed by drought, insect infestations, more frequent and severe windstorms, and intensified wildfire regimes (Caldwell et al., 2013; Litschert et al., 2012; Wohl, 2013c). Large wood recruited to the channel and floodplain by individual or mass tree mortality is less likely to be mobilized in the absence of high or sustained peak flows, which may increase OC storage in the form of large wood.

7. Conclusion

Mountainous headwater streams are important components of the terrestrial carbon cycle, contributing to carbon storage and ecosystem productivity. Results presented here indicate that OC storage along river corridors of the CFR is higher in relatively unconfined valleys, in low-gradient valleys, and at higher elevations. Within unconfined valleys, single-thread channels store more OC per area than complex, multithread channels. We attribute greater OC storage in single-thread channels within unconfined valleys to the dissipation of energy along elevated, cohesive, and grass-dominated floodplains that promote the aggradation of fine sediment and OC. In contrast, persistent channel-spanning logjams that promote the development of multithread planforms also reduce floodplain fine sediment aggradation. We posit that decreased flow depth and partitioning of shear stress across logjams and numerous channels of flow facilitate selective transport of fine sediment and OM. These processes limit fine sediment aggradation and the magnitude of OC storage per unit area. Shallower fine sediment storage and increased microbial transformation of OM reduce OC storage in floodplains of multithread channels. Although multithread channels do not store the most OC per area, they serve as hotspots for OM transformation, and provide critical energy sources that fuel downstream aquatic food webs. These results suggest that valley geometry and channel complexity coregulate OC-storage responses to observed increases in flood frequency, predicted increases in flood magnitude, and anticipated losses in hydrologic connectivity within fluvial systems. The effects of valley geometry and channel complexity on OM transformation and storage suggests that contemporary efforts to restore river-wetland systems (Powers et al., 2019) by reintroducing large wood to channels (Grabowski et al., 2019; Roni et al., 2014) will affect the storage and transformation of organic carbon along river corridors.

Data Availability Statement

All data generated in this study can be accessed through the associated Supporting Information file, http://hdl.handle.net/10217/173334, and Sutfin (2020) cited below.

Acknowledgments
This study is based upon work supported by National Science Foundation Grant No. DGE-0966346 "I-WATER: Integrated Water, Atmosphere, Ecosystems Education and Research Program" at Colorado State University (CSU); NSF Doctoral Research Dissertation Improvement Grant #1536186; and graduate student research grants from the Geological Society of America, the Colorado Scientific Society, and the Colorado State University Warner College of Natural Resources and Department of Geosciences. The authors thank Rocky Mountain National Park for their support and research permits, Teagan Deeney, and Jim Self at the CSU Soil and Water Laboratory, Mark Pascke for use of his lab, Thomas Borch for his insight and guidance, and assistance in the field and the laboratory by Ben Von Thaden, Dean Anderson, John Harris, Matheus Cruz Lima Pereira, Bryce Johnson, Julia Makiejus, Pamela Wagener, Jon Garber, Joel Sholtes, and Fernando Javier Ugalde Pascual.

References

Akaike, H. (1998). A New Look at the Statistical Model Identification. In E. Parzen, K. Tanabe, & G. Kitagawa (Eds.), *Selected papers of Hirotugu Akaike* (pp. 215–222). New York, NY: Springer New York. https://doi.org/10.1007/978-1-4612-1694-0_16

Alexander, L., Autrey, B., DeMeester, J., & Fritz, K. M. (2015). *Connectivity of streams and wetlands to downstream waters: A review and synthesis of the scientific evidence* (p. 408). The U.S. Environmental Protection Agency's (USEPA) Office of Research and Development.

Anderson, R. S., Riihimaki, C. A., Safran, E. B., & MacGregor, K. R. (2006). Facing reality: Late Cenozoic evolution of smooth peaks, glacially ornamented valleys, and deep river gorges of Colorado's front range. *Special paper of the geological society of America*, *398*, 397–418. https://doi.org/10.1130/2006.2398(25)

Aufdenkampe, A. K., Mayorga, E., Raymond, P. A., Melack, J. M., Doney, S. C., Alin, S. R., et al. (2011). Riverine coupling of biogeochemical cycles between land, oceans, and atmosphere. *Frontiers in Ecology and the Environment*, *9*, 53–60. https://doi.org/10.1890/100014

Ballantyne, A. P., Alden, C. B., Miller, J. B., Tans, P. P., & White, J. W. C. (2012). Increase in observed net carbon dioxide uptake by land and oceans during the past 50 years. *Nature*, *488*(7409), 70–72. https://doi.org/10.1038/nature11299

Barry, R. G. (1973). A climatological transect on the east slope of the Front Range, Colorado. *Arctic and Alpine Research*, *5*, 89–110. https://doi.org/10.1080/00040851.1973.1200368410.2307/1550251

Bates, B., Kundzewicz, Z. W., Wu, S., & Palutikof, J. (2008). *Climate change and water*. Technical paper of the intergovernmental panel on climate change (technical paper VI no. VI) (p. 210). Geneva: IPCC Secretariat. Retrieved from https://digital.library.unt.edu/ark:/67531/metadc11958/m1/13/

Battin, T. J., Kaplan, L. A., Findlay, S., Hopkinson, C. S., Marti, E., Packman, A. I., et al. (2008). Biophysical controls on organic carbon fluxes in fluvial networks. *Nature Geoscience*, *1*, 95–100. https://doi.org/10.1038/ngeo101

Beckman, N. D., & Wohl, E. (2014). Carbon storage in mountainous headwater streams: The role of old-growth forest and logjams. *Water Resources Research*, *50*, 2376–2393. https://doi.org/10.1002/2013WR014167

Birkeland, P. W., Shroba, R. R., Burns, S. F., Price, A. B., & Tonkin, P. J. (2003). Integrating soils and geomorphology in mountains: An example from the Front Range of Colorado. *Geomorphology*, *55*(1), 329–344. https://doi.org/10.1016/S0169-555X(03)00148-X

Blum, A. G., Ferraro, P. J., Archfield, S. A., & Ryberg, K. R. (2020). Causal effect of impervious cover on annual flood magnitude for the United States. *Geophysical Research Letters*, *47*, e2019GL086480. https://doi.org/10.1029/2019GL086480

Boye, K., Noël, V., Tfaily, M. M., Bone, S. E., Williams, K. H., Bargar, J. R., & Fendorf, S. (2017). Thermodynamically controlled preservation of organic carbon in floodplains. *Nature Geoscience*, *10*, 415–419. https://doi.org/10.1038/ngeo2940

Braddock, W. A., & Cole, J. C. (1990). *Geologic map of Rocky mountain National Park and vicinity, Colorado*. U.S. Geological Survey. https://doi.org/10.3133/i1973

Brown, A. G., Lespez, L., Sear, D. A., Macaire, J.-J., Houben, P., Klimek, K., et al. (2018). Natural vs anthropogenic streams in Europe: History, ecology and implications for restoration, river-rewilding and riverine ecosystem services. *Earth-Science Reviews*, *180*, 185–205. https://doi.org/10.1016/j.earscirev.2018.02.001

Cadol, D., & Wohl, E. (2011). Coarse sediment movement in the vicinity of a logjam in a neotropical gravel-bed stream. *Geomorphology*, *128*, 191–198. https://doi.org/10.1016/j.geomorph.2011.01.007

Caldwell, M. K., Hawbaker, T. J., Briggs, J. S., Cigan, P. W., & Stitt, S. (2013). Simulated impacts of mountain pine beetle and wildfire disturbances on forest vegetation composition and carbon stocks in the Southern Rocky Mountains. *Biogeosciences*, *10*, 8203–8222. https://doi.org/10.5194/bg-10-8203-2013

Chapin, F. S., Matson, P. A., & Vitousek, P. (2011). *Principles of terrestrial ecosystem ecology* (2nd ed.). New York, NY: Springer Science & Business Media. https://doi.org/10.1007/978-1-4419-9504-9

Chen, W., Westerhoff, P., Leenheer, J. A., & Booksh, K. (2003). Fluorescence excitation: Emission matrix regional integration to quantify spectra for dissolved organic matter. *Environmental Science & Technology*, *37*(24), 5701–5710. https://doi.org/10.1021/es034354c

Collins, B. D., Montgomery, D. R., Fetherston, K. L., & Abbe, T. B. (2012). The floodplain large-wood cycle hypothesis: A mechanism for the physical and biotic structuring of temperate forested alluvial valleys in the North Pacific coastal ecoregion. *Geomorphology*, *139-140*, 460–470. https://doi.org/10.1016/j.geomorph.2011.11.011

Danczak, R. E., Sawyer, A. H., Williams, K. H., Stegen, J. C., Hobson, C., & Wilkins, M. J. (2016). Seasonal hyporheic dynamics control coupled microbiology and geochemistry in Colorado River sediments. *Journal of Geophysical Research: Biogeosciences*, *121*(12), 2976–2987. https://doi.org/10.1002/2016JG003527

D'Elia, A. H., Liles, G. C., Viers, J. H., & Smart, D. R. (2017). Deep carbon storage potential of buried floodplain soils. *Scientific Reports*, *7*(1), 8181. https://doi.org/10.1038/s41598-017-06494-4

Downing, J., Cole, J. J., Duarte, C. M., Middelburg, J. J., Melack, J. M., Prairie, Y. T., et al. (2012). Global abundance and size distribution of streams and rivers. *Inland Waters*, *2*, 229–236. https://doi.org/10.5268/IW-2.4.502

Dunne, T., & Leopold, L. B. (1978). *Water in environmental planning* (p. 818). Macmillan.

Falkowski, P., Scholes, R. J., Boyle, E., Canadell, J., Canfield, D., Elser, J., et al. (2000). The global carbon cycle: A test of our knowledge of earth as a system. *Science*, *290*, 291–296. https://doi.org/10.1126/science.290.5490.291

Fellman, J. B., Hood, E., & Spencer, R. G. M. (2010). Fluorescence spectroscopy opens new windows into dissolved organic matter dynamics in freshwater ecosystems: A review. *Limnology & Oceanography*, *55*, 2452–2462. https://doi.org/10.4319/lo.2010.55.6.2452

FIA. (2019). *Forest inventory and analysis national Program: FIA library*. Washington, D.C: U.S. Forest Service, FIA Program. Retrieved from https://www.fia.fs.fed.us/library/field-guides-methods-proc/

Galy, V., Peucker-Ehrenbrink, B., & Eglinton, T. (2015). Global carbon export from the terrestrial biosphere controlled by erosion. *Nature*, *521*, 204–207. https://doi.org/10.1038/nature14400

Glass, S. V., & Zelinka, S. L. (2004). *Wood handbook Ch 4: Moisture relations and physical properties of wood (USDA general technical report no. FPL-GTR-190)* (p. 20). Madison, WI: U.S. Department of Agriculture, Forest Service, Forest Products Laboratory. Retrieved from https://www.fpl.fs.fed.us/documnts/fplgtr/fplgtr190/chapter_04.pdf

Gochis, D., Schumacher, R., Friedrich, K., Doesken, N., Kelsch, M., Sun, J., et al. (2014). The Great Colorado Flood of September 2013. *Bulletin of the American Meteorological Society*, *96*, 1461–1487. https://doi.org/10.1175/BAMS-D-13-00241.1

Gooseff, M. N., Hall, R. O., & Tank, J. L. (2007). Relating transient storage to channel complexity in streams of varying land use in Jackson Hole, Wyoming. *Water Resources Research*, *43*, W01417. https://doi.org/10.1029/2005WR004626

Grabowski, R. C., Gurnell, A. M., Burgess-Gamble, L., England, J., Holland, D., Klaar, M. J., et al. (2019). The current state of the use of large wood in river restoration and management. *Water and Environment Journal*, *33*, 366–377. https://doi.org/10.1111/wej.12465

Gregory, J. M., Jones, C. D., Cadule, P., & Friedlingstein, P. (2009). Quantifying Carbon Cycle Feedbacks. *Journal of Climate*, *22*, 5232–5250. https://doi.org/10.1175/2009JCLI2949.1

Gudmundsson, L., Leonard, M., Do, H. X., Westra, S., & Seneviratne, S. I. (2019). Observed Trends in Global Indicators of Mean and Extreme Streamflow. *Geophysical Research Letters*, *46*, 756–766. https://doi.org/10.1029/2018GL079725

Herdrich, A. T., Winkelman, D. L., Venarsky, M. P., Walters, D. M., & Wohl, E. (2018). The loss of large wood affects rocky mountain trout populations. *Ecology of Freshwater Fish*, *27*(4), 1023–1036. https://doi.org/10.1111/eff.12412

Hirsch, R. M., & Archfield, S. A. (2015). Not higher but more often. *Nature Climate Change*, *5*, 198–199. https://doi.org/10.1038/nclimate2551

Hoffmann, T., Glatzel, S., & Dikau, R. (2009). A carbon storage perspective on alluvial sediment storage in the Rhine catchment. *Geomorphology*, *108*, 127–137. https://doi.org/10.1016/j.geomorph.2007.11.015

Hupp, C. R., Kroes, D. E., Noe, G. B., Schenk, E. R., & Day, R. H. (2019). Sediment trapping and carbon sequestration in floodplains of the lower Atchafalaya Basin, LA: Allochthonous versus autochthonous carbon sources. *Journal of Geophysical Research: Biogeosciences*, *124*, 663–677. https://doi.org/10.1029/2018JG004533

Ives, R. L. (1942). The beaver-meadow complex. *Journal of Geomorphology*, *5*(3), 191–203

Jarrett, R. D. (1990). Paleohydrologic techniques used to define the spatial occurrence of floods. *Geomorphology*, *3*, 181–195. https://doi.org/10.1016/0169-555X(90)90044-Q

Kampf, S. K., & Lefsky, M. A. (2016). Transition of dominant peak flow source from snowmelt to rainfall along the Colorado Front Range: Historical patterns, trends, and lessons from the 2013 Colorado Front Range floods. *Water Resources Research*, *52*, 407–422. https://doi.org/10.1002/2015WR017784

Kubista, M., Sjöback, R., Eriksson, S., & Albinsson, B. (1994). Experimental correction for the inner-filter effect in fluorescence spectra. *Analyst*, *119*, 417–419. https://doi.org/10.1039/AN9941900417

Laurel, D., & Wohl, E. (2019). The persistence of beaver-induced geomorphic heterogeneity and organic carbon stock in river corridors. *Earth Surface Processes and Landforms*, *44*, 342–353. https://doi.org/10.1002/esp.4486

Lawaetz, A. J., & Stedmon, C. A. (2009). Fluorescence intensity calibration using the Raman scatter peak of water. *Applied Spectroscopy*, *63*, 936–940. https://doi.org/10.1366/000370209788964548

Lininger, K. B., & Wohl, E. (2019). Floodplain dynamics in North American permafrost regions under a warming climate and implications for organic carbon stocks: A review and synthesis. *Earth-Science Reviews*, *193*, 24–44. https://doi.org/10.1016/j.earscirev.2019.02.024

Lininger, K. B., Wohl, E., Rose, J. R., & Leisz, S. J. (2019). Significant floodplain soil organic carbon storage along a large high-latitude river and its tributaries. *Geophysical Research Letters*, *46*, 2121–2129. https://doi.org/10.1029/2018GL080996

Litschert, S. E., Brown, T. C., & Theobald, D. M. (2012). Historic and future extent of wildfires in the Southern Rockies Ecoregion, USA. *Forest Ecology and Management*, *269*, 124–133. https://doi.org/10.1016/j.foreco.2011.12.024

Livers, B., & Wohl, E. (2015). An evaluation of stream characteristics in glacial versus fluvial process domains in the Colorado Front Range. *Geomorphology*, *231*, 72–82. https://doi.org/10.1016/j.geomorph.2014.12.003

Livers, B., & Wohl, E. (2016). Sources and interpretation of channel complexity in forested subalpine streams of the Southern Rocky Mountains. *Water Resources Research*, *52*, 3910–3929. https://doi.org/10.1002/2015WR018306

Livers, B., Wohl, E., Jackson, K. J., & Sutfin, N. A. (2018). Historical land use as a driver of alternative states for stream form and function in forested mountain watersheds of the Southern Rocky Mountains. *Earth Surface Processes and Landforms*, *43*, 669–684. https://doi.org/10.1002/esp.4275

Lynch, L. M., Machmuller, M. B., Boot, C. M., Covino, T. P., Rithner, C. D., Cotrufo, M. F., et al. (2019a). Dissolved organic matter chemistry and transport along an Arctic tundra hillslope. *Global Biogeochemical Cycles*, *33*. https://doi.org/10.1029/2018GB006030

Lynch, L. M., Sutfin, N. A., Fegel, T. S., Boot, C. M., Covino, T. P., & Wallenstein, M. D. (2019b). River channel connectivity shifts metabolite composition and dissolved organic matter chemistry. *Nature Communications*, *10*(1), 459. https://doi.org/10.1038/s41467-019-08406-8

Manga, M., & Kirchner, J. W. (2000). Stress partitioning in streams by large woody debris. *Water Resources Research*, *36*, 2373–2379. https://doi.org/10.1029/2000WR900153

McCain, J. F, & Shroba, R. R (1979). *Storm and flood of July 31-August 1, 1976, in the Big Thompson River and Cache la Poudre River basins, Larimer and Weld Counties, Colorado (USGS numbered series No. 1115- A,B)*. U.S. Govt. Print. Off. https://doi.org/10.3133/pp1115ab

Montgomery, D. R., & Buffington, J. M. (1997). Channel-reach morphology in mountain drainage basins. *Geological Society of America Bulletin*, *109*, 596–611. https://doi.org/10.1130/0016-7606(1997)109<0596:CRMIMD>2.3.CO;2

Moody, J. A., & Ebel, B. A. (2012). Hyper-dry conditions provide new insights into the cause of extreme floods after wildfire. *Catena*, *93*, 58–63. https://doi.org/10.1016/j.catena.2012.01.006

Omengo, F. O., Geeraert, N., Bouillon, S., & Govers, G. (2018). Deposition and fate of organic carbon in floodplains along a tropical semiarid lowland river (Tana River, Kenya). *Journal of Geophysical Research: Biogeosciences*, 1131–1143. https://doi.org/10.1002/2015JG003288@10.1002/(ISSN)2169-8961.CNFLOI1

Poff, N. L., Allan, J. D., Bain, M. B., Karr, J. R., Prestegaard, K. L., Richter, B. D., et al. (1997). The natural flow regime. *BioScience*, *47*, 769–784. https://doi.org/10.2307/1313099

Polvi, L. E., & Wohl, E. (2012). The beaver meadow complex revisited - the role of beavers in post-glacial floodplain development. *Earth Surface Processes and Landforms*, *37*, 332–346. https://doi.org/10.1002/esp.2261

Polvi, L. E., & Wohl, E. (2013). Biotic drivers of stream planform. *BioScience*, *63*(6), 439–452. https://doi.org/10.1525/bio.2013.63.6.6

Polvi, L. E., Wohl, E. E., & Merritt, D. M. (2011). Geomorphic and process domain controls on riparian zones in the Colorado Front Range. *Geomorphology*, *125*, 504–516. https://doi.org/10.1016/j.geomorph.2010.10.012

Powers, P. D., Helstab, M., & Niezgoda, S. L. (2019). A process-based approach to restoring depositional river valleys to Stage 0, an anastomosing channel network. *River Research and Applications*, *35*, 3–13. https://doi.org/10.1002/rra.3378

PRISM Climate Group. (2012). *PRISM Climate Data*. Oregon State University. Retrieved from http://prism.oregonstate.edu

Rathburn, S. L., Bennett, G. L., Wohl, E. E., Briles, C., McElroy, B., & Sutfin, N. (2017). The fate of sediment, wood, and organic carbon eroded during an extreme flood, Colorado Front Range, USA. *Geology*, *45*, 499–502. https://doi.org/10.1130/G38935.1

Raymond, P. A., Saiers, J. E., & Sobczak, W. V. (2016). Hydrological and biogeochemical controls on watershed dissolved organic matter transport: Pulse-shunt concept. *Ecology*, *97*, 5–16. https://doi.org/10.1890/14-1684.1

R Core Team. (2017). *R: A language and environment for statistical computing*. Vienna, Austria: R Foundation for Statistical Computing. Retrieved from http://www.R-project.org/

Richter, B. D., Baumgartner, J. V., Powell, J., & Braun, D. P. (1996). A method for assessing hydrologic alteration within ecosystems. *Conservation Biology*, *10*, 1163–1174. https://doi.org/10.1046/j.1523-1739.1996.10041163.x

Ricker, M. C., & Lockaby, B. G. (2015). Soil organic carbon stocks in a large eutrophic floodplain forest of the southeastern Atlantic Coastal Plain, USA. *Wetlands*, *35*, 291–301. https://doi.org/10.1007/s13157-014-0618-y

Roni, P., Beechie, T., Pess, G., & Hanson, K. (2014). Wood placement in river restoration: Fact, fiction, and future direction. *Canadian Journal of Fisheries and Aquatic Sciences*, *72*, 466–478. https://doi.org/10.1139/cjfas-2014-0344

Scott, D. N., & Wohl, E. E. (2018). Geomorphic regulation of floodplain soil organic carbon concentration in watersheds of the Rocky and Cascade Mountains, USA. *Earth Surf. Dynam.*, *6*, 1101–1114. https://doi.org/10.5194/esurf-6-1101-2018

Sear, D. A., Millington, C. E., Kitts, D. R., & Jeffries, R. (2010). Logjam controls on channel: Floodplain interactions in wooded catchments and their role in the formation of multi-channel patterns. *Geomorphology*, *116*, 305–319. https://doi.org/10.1016/j.geomorph.2009.11.022

Sharma, A., Wasko, C., & Lettenmaier, D. P. (2018). If precipitation extremes are increasing, why aren't floods? *Water Resources Research*, *54*, 8545–8551. https://doi.org/10.1029/2018WR023749

Sholtes, J. S., Yochum, S. E., Scott, J. A., & Bledsoe, B. P. (2018). Longitudinal variability of geomorphic response to floods. *Earth Surface Processes and Landforms*, *43*, 3099–3113. https://doi.org/10.1002/esp.4472

Simon, A., & Collison, A. J. C. (2002). Quantifying the mechanical and hydrologic effects of riparian vegetation on streambank stability. *Earth Surface Processes and Landforms*, *27*, 527–546. https://doi.org/10.1002/esp.325

Stegen, J. C., Fredrickson, J. K., Wilkins, M. J., Konopka, A. E., Nelson, W. C., Arntzen, E. V., et al. (2016). Groundwater-surface water mixing shifts ecological assembly processes and stimulates organic carbon turnover. *Nature Communications*, *7*, 11237. https://doi.org/10.1038/ncomms11237

Stewart, I. T. (2009). Changes in snowpack and snowmelt runoff for key mountain regions. *Hydrological Processes*, *23*, 78–94. https://doi.org/10.1002/hyp.7128

Sutfin, N. (2020). *Floodplain organic carbon storage along streams in the Colorado Front Range, U.S.A*. https://doi.org/10.6084/m9.figshare.12014586.v110.1130/abs/2020am-359381

Sutfin, N. A., & Wohl, E. (2017). Substantial soil organic carbon retention along floodplains of mountain streams. *Journal of Geophysical Research: Earth Surface*, *122*, 1325–1338. https://doi.org/10.1002/2016JF004004

Sutfin, N. A., & Wohl, E. (2019). Elevational differences in hydrogeomorphic disturbance regime influence sediment residence times within mountain river corridors. *Nature Communications*, *10*, 2221. https://doi.org/10.1038/s41467-019-09864-w

Sutfin, N. A., Wohl, E. E., & Dwire, K. A. (2016). Banking carbon: A review of organic carbon storage and physical factors influencing retention in floodplains and riparian ecosystems. *Earth Surface Processes and Landforms*, *41*, 38–60. https://doi.org/10.1002/esp.3857

Tabari, H. (2020). Climate change impact on flood and extreme precipitation increases with water availability. *Scientific Reports*, *10*, 13768. https://doi.org/10.1038/s41598-020-70816-2

Vannote, R. L., Minshall, G. W., Cummins, K. W., Sedell, J. R., & Cushing, C. E. (1980). The river continuum concept. *Canadian Journal of Fisheries and Aquatic Sciences*, *37*, 130–137. https://doi.org/10.1139/f80-017

Veblen, T. T., & Donnegan, J. (2005). *Historical range of variability for forest vegetation of the national forests of the Colorado Front Range* (p. 154). Golden, CO: USDA Forest Service, Rocky Mountain Region.

Venarsky, M. P., Walters, D. M., Hall, R. O., Livers, B., & Wohl, E. (2018). Shifting stream planform state decreases stream productivity yet increases riparian animal production. *Oecologia*, *187*, 167–180. https://doi.org/10.1007/s00442-018-4106-6

Weishaar, J. L., Aiken, G. R., Bergamaschi, B. A., Fram, M. S., Fujii, R., & Mopper, K. (2003). Evaluation of specific ultraviolet absorbance as an indicator of the chemical composition and reactivity of dissolved organic carbon. *Environmental Science & Technology*, *37*, 4702–4708. https://doi.org/10.1021/es030360x

Wohl, E. (2008). The effect of bedrock jointing on the formation of straths in the Cache la Poudre River drainage, Colorado Front Range. *Journal of Geophysical Research*, *113*. https://doi.org/10.1029/2007JF000817

Wohl, E. (2013a). Landscape-scale carbon storage associated with beaver dams. *Geophysical Research Letters*, *40*, 3631–3636. https://doi.org/10.1002/grl.50710

Wohl, E. (2013b). *Mountain rivers revisited*. Washington, D.C.: American Geophysical Union Press.

Wohl, E. (2013c). Redistribution of forest carbon caused by patch blowdowns in subalpine forests of the Southern Rocky Mountains, USA. *Global Biogeochemical Cycles*, *27*, 1205–1213. https://doi.org/10.1002/2013GB004633

Wohl, E. (2020). Wood process domains and wood loads on floodplains. *Earth Surface Processes and Landforms*, *45*, 144–156. https://doi.org/10.1002/esp.4771

Wohl, E., Bledsoe, B. P., Jacobson, R. B., Poff, N. L., Rathburn, S. L., Walters, D. M., & Wilcox, A. C. (2015). The natural sediment regime in rivers: Broadening the foundation for ecosystem management. *BioScience*, *65*, 358–371. https://doi.org/10.1093/biosci/biv002

Wohl, E., & Cadol, D. (2011). Neighborhood matters: Patterns and controls on wood distribution in old-growth forest streams of the Colorado Front Range, USA. *Geomorphology*, *125*, 132–146. https://doi.org/10.1016/j.geomorph.2010.09.008

Wohl, E., Dwire, K., Sutfin, N., Polvi, L., & Bazan, R. (2012). Mechanisms of carbon storage in mountainous headwater rivers. *Nature Communications*, *3*, 1263. https://doi.org/10.1038/ncomms2274

Wohl, E., Lininger, K. B., & Scott, D. N. (2017). River beads as a conceptual framework for building carbon storage and resilience to extreme climate events into river management. *Biogeochemistry*, *141*, 365–383. https://doi.org/10.1007/s10533-017-0397-7

Wohl, E., & Scamardo, J. E. (2021). The resilience of logjams to floods. *Hydrological Processes*, *35*, e13970. https://doi.org/10.1002/hyp.13970

Wollheim, W. M., Bernal, S., Burns, D. A., Czuba, J. A., Driscoll, C. T., Hansen, A. T., et al. (2018). River network saturation concept: factors influencing the balance of biogeochemical supply and demand of river networks. *Biogeochemistry*, *141*, 503–521. https://doi.org/10.1007/s10533-018-0488-0

Yochum, S. E., & Collins, F. (2015). Colorado front range flood of 2013: peak flows and flood frequencies. *3rd joint federal interagency conference on sedimentation and hydrologic modeling*. Reno, Nevada, USA. https://doi.org/10.13140/RG.2.1.3439.1520

Yochum, S. E., Sholtes, J. S., Scott, J. A., & Bledsoe, B. P. (2017). Stream power framework for predicting geomorphic change: The 2013 Colorado Front Range flood. *Geomorphology*, *292*, 178–192. https://doi.org/10.1016/j.geomorph.2017.03.004